AD NUMBER
ADA180294
LIMITATION CHANGES
TO: **Approved for public release; distribution is unlimited. Document partially illegible.**
FROM: **Distribution authorized to U.S. Gov't. agencies and their contractors; Administrative/Operational Use; AUG 1986. Other requests shall be referred to Office of Naval Research, Washington, DC. Document partially illegible.**
AUTHORITY
per onr/code 1131 ltr, dtd 30 apr 1987

PROGRESS REPORT

STUDIES OF ICOSAHEDRAL QUASICRYSTALS

D. Shechtman and E. Horowitz

Submitted by: The Johns Hopkins University
G.W.C. Whiting School of Engineering
Materials Science and Engineering Department
Baltimore, Maryland 21218
Attn: E. Horowitz (301)338-7916

DARPA Order No. 5527 (5-30-85)
ONR Order No. N00014-85-K-0779
Effective Date: 08-01-85
Expiration Date: 06-30-87
Sponsored By: Defense Research Projects Agency (DARPA)
and The Office of Naval Research (ONR)

August 1986

DISCLAIMER NOTICE

THIS DOCUMENT IS BEST QUALITY PRACTICABLE. THE COPY FURNISHED TO DTIC CONTAINED A SIGNIFICANT NUMBER OF PAGES WHICH DO NOT REPRODUCE LEGIBLY.

PROGRESS REPORT

STUDIES OF ICOSAHEDRAL QUASICRYSTALS

D. Shechtman and E. Horowitz

Submitted by: The Johns Hopkins University
G.W.C. Whiting School of Engineering
Materials Science and Engineering Department
Baltimore, Maryland 21218
Attn: E. Horowitz (301)338-7916

DARPA Order No. 5527 (5-30-85)
ONR Order No. N00014-85-K-0779
Effective Date: 08-01-85
Expiration Date: 06-30-87
Sponsored By: Defense Research Projects Agency (DARPA)
and The Office of Naval Research (ONR)

August 1986

Table of Contents

Executive Summary

The five manuscripts reproduced in this progress report cover the research of the Principal Investigator, Dr. Dan Shechtman, and his collaborators under the DARPA/ONR sponsored research program on icosahedral quazicrystals formed by rapid solidification of alloys. First, microscopic evidence for quasi-periodicity in an alloy with long-range icosahedral order is presented. Local 5-fold rotational axes are observed to be uniformly distributed down to the atomic scale. Twinning and modulated structures are ruled out based on the experimental data.

In a high resolution electron microscopy study on rapidly solidified Al_6Mn alloy ribbons the relevant characteristics of quasi-periodicity were demonstrated. The particular topological properties of such a periodic network are best observed by direct imaging of the quasi-lattice in the electron microscope.

The indexing of icosahedral quasiperiodic crystals is described by Cahn, Shechtman and Gratias including the step necessary to prove, by diffraction, that an object is quasiperiodic. Various coordinate systems are discussed and an explanation is given for choosing one aligned with a set of three orthogonal two-fold axes. Using this coordinate system the main crystallographic projections are presented and several analyzed single-crystal electron diffraction patterns are demonstrated.

In another manuscript Shechtman provides experimental evidence for quasiperiodic crystals. The experiments include various diffraction techniques for studying the long-range order as well as the methods to determine the local atomic order. The diffraction pattern has well defined sharp peaks and fivefold rotational symmetry and the crystals, in different orientations, have more of these five fold diffraction patterns. The lattice imaging technique was used extensively to study lattice defects. The technique can be used to detect the fine structure of dislocation cores and microtwin boundaries. No boundaries were seen in the samples under investigation while the quasiperiodic sequence of planes is clearly visible.

Neutron diffraction was used by Mozer, Cahn, Gratias and Shechtman to investigate the icosahedral phase of aluminum-manganese alloys. All the peaks appear at the angles in agreement with the icosahedral indexing with a six-dimensional cubic lattice parameter of approximately 0.65 mm. that decreased with increasing Mn content.

The research results furnish additional strong documentation for the existence of the icosahedral quasicrystals. A variety of characterization techniques are described and the experimental data is analyzed and explained. The work advances our knowledge and understanding of quasicrystals and their relationship to chemical composition and solidification conditions.

MICROSCOPIC EVIDENCE FOR QUASI-PERIODICITY IN A SOLID WITH LONG-RANGE ICOSAHEDRAL ORDER.

Abstract:

High resolution electron microscopy images of an icosahedral solid reveal many of the important geometrical characteristics of quasi-periodicity. In addition, the local 5-fold rotational axes are seen to be uniformly distributed down to the atomic scale; we find no evidence of an underlying 3-dimensional lattice, thereby ruling out the hypotheses of microtwinning and modulated structures.

D. SHECHTMAN Department of Materials Engineering, Israel Institut of Technology, Technion, 32000 HAIFA ISRAEL and Materials Science and Engineering Department, Johns Hopkins University, Baltimore, Maryland 21218, U.S.A.

D. GRATIAS C.E.C.M./C.N.R.S. 15 rue G. Urbain 94400 VITRY, FRANCE

J. W. CAHN Center for Materials Science, National Bureau of Standards, GAITHERSBURG, MD 20899, U.S.A.

C.R. Acad. Sci. Paris, T300, Series II, No. 18, 909-14 (1985).

We recently reported (1,2) the existence of a metallic solid with long-range orientational order which produces sharp diffraction like a crystal, but whose point group (icosahedral m35) is inconsistent with any translation symmetry in 3-dimensional space. Discrete diffraction results not only from strict periodicity but from a more general and less restrictive property called the "quasi-periodicity" (or "almost-periodicity"). Structures which are quasi-periodic may exhibit any kind of point symmetry including five-fold symmetry(4,5,6,7).In this note, we present experimental evidence that the alloy Al6Mn rapidly solidified is indeed a quasi-periodic icosahedral solid and thereby rule out several alternate proposals such as microtwinning (8) and incommensurate modulated structures (9). Our conclusions are based on the sole hypothesis that high resolution images in electron microscopy show the same topological properties as the projected potential of the structure.

The observations were made on a rapidly solidified ribbon of the composition Al-14.3 a/o Mn. Electron microscopy was performed on a JEOL 200CX microscope equiped with a ultra-high resolution polar piece and a goniometer stage. Shown on Figure 1 is a single high resolution image oriented along a five-fold axis,the corresponding diffraction pattern and the optical Fourier transform of the image. The indexing of the diffraction pattern requires the

introduction of six indices, two per independent unit vectors,the fisrt one associated with integer length, the second one with the irrational length corresponding to the golde mean τ (τ=1.618034...),an algebraic irrational number equal to $2\cos\pi/5$ and therefore directly induced by the five-fold symmetry (10). A discrete Fourier spectrum with a finite number of integer indices but greater than the dimensionality defines a structure to be quasi-periodic(3). An important property of the quasi-periodicity results in the unusual progressing of the intensities of the reflections. More and more intense reflections occur at distances $n+m\tau$ in which m/n are the successive convergent approximants of τ . The geometrical properties of quasiperiodic patterns have extensively studied these last years (for a general survey of aperiodic tilings see reference 11); rigourous algebraic derivations are now proposed (12,13,14) which generalize the original Penrose tilings (4). All patterns of five-fold symmetry exhibit essential characteristics like Fibonacci sequences and invariance through homothetic multiplication by the golden mean.

The high resolution image has indeed all the essential properties of a two-dimensional generalized Penrose tiling: short Fibonacci sequences of two fundamental lengths related by the golden mean are identified both in the spacing of rows and in the spacing of bright spots within rows; also

the same sequences and patterns occur at several different scales of length. This is particularly clear for pentagons of bright spots which interpenetrate at larger and larger scales. Although there is no strict periodicity, any finite feature on the micrograph is found repeated and oriented the same way at some finite (but not constant!) distance. This property constitutes the essence of quasi-periodic patterns which are the" most periodic" among the aperiodic patterns. We therefore conclude that we are seeing in Figure 1 a projection along a five-fold axis of a quasi-periodic 3-dimensional structure with icosahedral symmetry. This conclusion is consistent with the recent illuminating mathematical derivation of Katz and Duneau (14) who demonstrated that the cuts along all high symmetry orientations (two-, three- and five-fold axes) of an icosahedral quasi-lattice are indeed 2-dimensional quasi-lattices. A complete report of the imaging of all high symmetry zones in high resolution microscopy will be published elsewhere (15).

The structural homogeneity of the icosahedral phase down to the atomic scale definitely contradicts the hypothesis of microtwinning in the sense in which this concept is commonly used. If microtwinning is redefined to include twinning of a size below the resolution of this microscope, the concept will have acquired a new meaning, which would raise more questions than it would solve. It

would still have to explain the long range orientational order, the typical Fibonacci sequences, the spatial self-similarity, as well as the unusual diffraction intensities which are perfectly well reproduced in kinematical calculations based on quasi-periodicity (13,14,15).

Weak beam electron microscopy does reveal a mottling in the 5nm range. This has been interpreted as evidence for the presence of microcrystals and hence of twinning (8); from our high resolution study we attribute this contrast mottling to the local variations of strains; this is confirmed by a continuous tilting experiment in the microscope: the bright area in dark field images move smoothly with no discontinuity.

A more subtle problem is the distinction between this structure and incommensurately modulated structures. We found no evidence of an underlying lattice in direct space which is consistent, in the reciprocal space, with the fact that the diffraction pattern can not be partitioned into "main" and "satellite" reflections. As far as the mathematical aspects are concerned, any quasi-periodic function, including one with icosahedral symmetry, may be regarded as the diagonal cut of a purely periodic function of N variables where N is the dimension of the algebraic base (here N=3x2). Accordingly, Janner and Janssen (16)

have shown that Z-modules in N dimensions (N>3) are the natural extension of the notion of crystal. At that point it seems useful to propose a scheme for classification of crystals.

A general diagonal cut will produce an incommensurate phase with irrational indices. The incommensuration varies with the angle of the cut. In real crystals, the incommensuration varies with temperature and composition and always results in a lowering of symmetry.

Special cuts give rise to higher symmetries: this is the case for orientations of the N-dimensional space which correspond to isolated strata: as a result the incommensuration is locked to a fixed cut angle and cannot vary with temperature and composition. This is the case for the icosahedral phase which, in fact, corresponds to a special cut of a 6-dimensional simple cubic (10,14). These special properties set the icosahedral phase into a particular class of modulated structures, the one that corresponds to isolated strata whose little groups do not belong to the 32 crystallographic point groups: the icosahedral phase is a "special point" long range ordered phase with noncrystallographic little group. This analysis suggests that the icosahedral phase could be a STABLE phase under certain conditions of composition temperature and pressure exactly like usual crystalline phases.

References

1. D. Shechtman and I. Blech, Met. Trans. accepted (1985).

2. D. Shechtman, I. Blech, D. Gratias and J.W. Cahn, Phys. Rev. Lett. 53,1951 -1954 (1984).

3. see, for instance, A. S. Besicovitch "Almost periodic functions", Cambridge, 1932.

4. R.Penrose, Math. Intell. 2, 32-37 (1979).

5. A. L. Mackay, Sov. Phys. Crystallogr. 26, 517-522 (1981).

6. P. Kramer and R. Neri, Acta Cryst. A40, 580-587 (1984).

7. D. Levine and P. Steinhardt Phys. Rev. Lett. 53,2477 (1934).

8. R. D. Field and H. L. Frazer, Mat. Sci. Eng. 68,L17 (1984-5).

9. P. Bak, submitted to Phys. Rev. Lett.

10. D. Shechtman, D. Gratias and J. W. Cahn submitted to Acta Cryst. A.

11. B. Grunbaum and G. C. Shephard " Tilings and Patterns", Freeman Ed., to be published.

12. N. G. de Bruijn, Ned. Akad. Wetensch. Proc. Ser. A43, 39-66 (1981).

13. A. Katz and M. Duneau, Workshop on Mathematical Crystallography, M. Senechal and L. Michel Ed., Institut des Hautes Etudes Scientifiques, Gif sur Yvette, January 1985.

14. M. Duneau and A. Katz submitted to Phys. Rev. Lett.

15. D. Shechtman, D. Gratias, R. Portier and J. W. Cahn submitted to Acta Cryst A.

16. A. Janner and T. Janssen, Physica B and C (Netherlands) 99B and C, No 1-4, 334-336 (1980).

Figure Captions

Figure 1: (a) Electron diffraction of the 5-fold ($1\bar{\tau}\,0$) zone axis.

(b)Corresponding high resolution image.

(c)Optical Fourier transform of (b) showing the restoration of the five-fold symmetry.

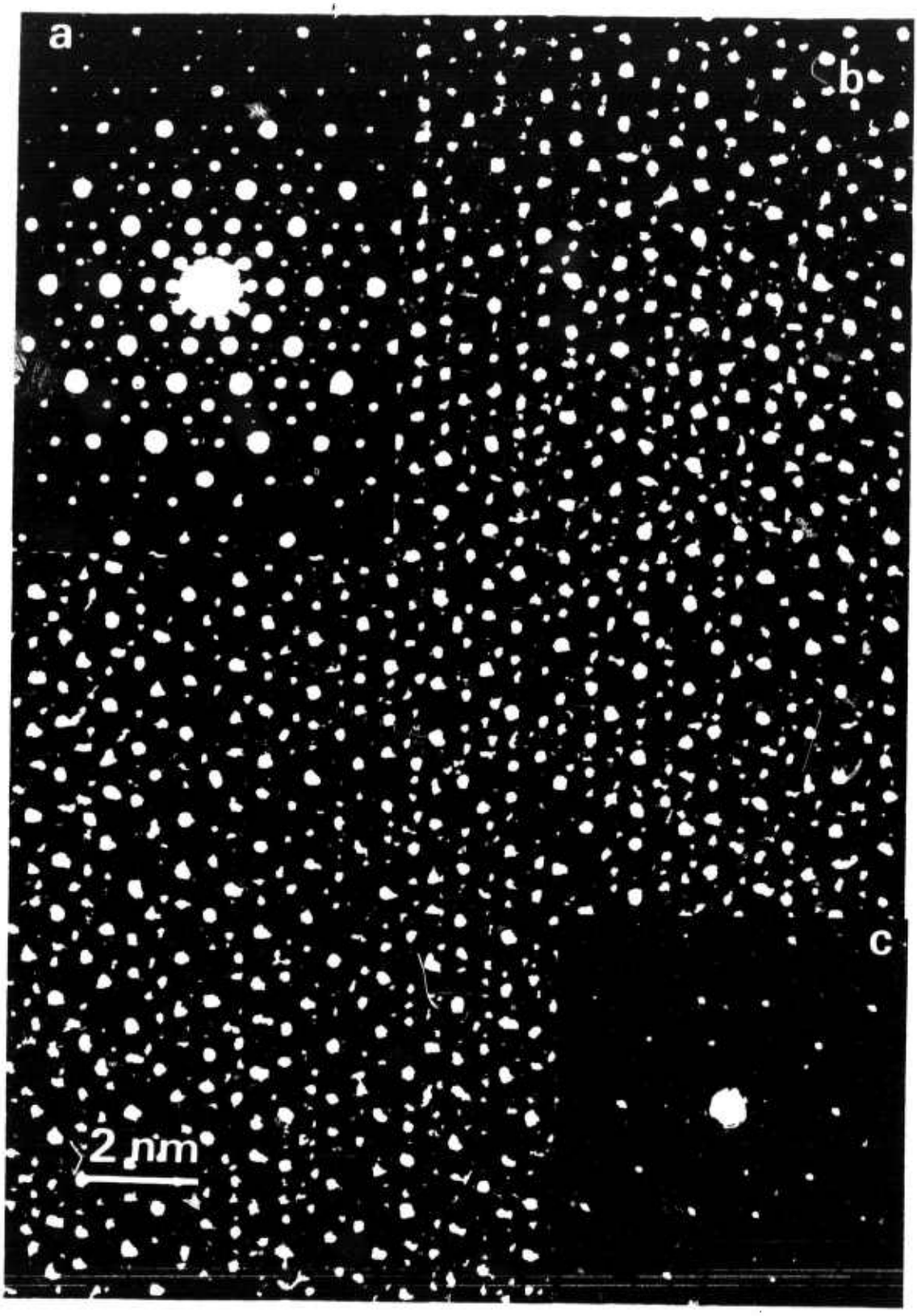
a
b
c
2 nm

High Resolution Electron Microscopy of Aluminum-based Icosahedral Quasi-Crystals

R. Portier(1), D. Shechtman(2), D. Gratias(1), J. Bigot(1) and J.W. Cahn(3).
(1) C.E.C.M./C.N.R.S. 15,rue G. Urbain 94400-Vitry/France.
(2) Dept of Mat. Eng., Israel Institut of Technology, Technion,32000 HAIFA, Israel.
Dept. of Materials Science and Engineering, Johns Hopkins University, Baltimore, Maryland U.S.A.
(3) Center of Mat. Sci., N.B.S., Gaithersburg, MD-20899, U.S.A.

Introduction.

Some rapidly solidified binary and ternary alloys exhibit a long range ordered structure with no translational periodicity (Shechtman et al 1984, 1985,Zhang et al to appear) but with a discrete Fourier spectrum characteristic of Almost-periodicity (Besicovith 1932). These have been recently called "quasi-crystals" (Levine et al 1985) and can be described by the Cut and Projection Method (C.P.M.) (Duneau et al 1985, Elser to appear, Kalugin et al 1985) which is a generalized discrete version of the earlier hyperspace description used for continuous density functions of incommensurate structures (Janssen et al 1984). The particular topological properties of such aperiodic networks are best observed by direct imaging of the quasi-lattice in the electron microscope. It is shown here that the relevant characteristics of quasi-periodicity are present in the images which can be interpreted independently from the actual organization of the atomic species within the quasi-periodic framework.

Experimental.

The observations reported here were made on rapidly solidified ribbons of the Al6Mn alloy. Electron microscopy was performed on a JEOL 200CX provided with the Cs=1mm pole piece and the $\pm$ 10° goniometer stage. The HR images along a five-fold axis are shown on Fig.1 for different defocus values and objective apertures .Although the images show no rigourous five-fold symmetry (only the Patterson of the structure does show an exact icosahedral symmetry) numerous homogeneously distributed pentagons and decagons are observed at atomic scale. White dots in Fig.1-a fit remarkably well with the simple projection of the quasi-lattice generated by C.P.M.; this is confirmed by Fig.2 which corresponds to the very important two-fold orientation.

J. Spectroscopie et Microscopie Electronique, 10, No. 2, 107-16 (1985).

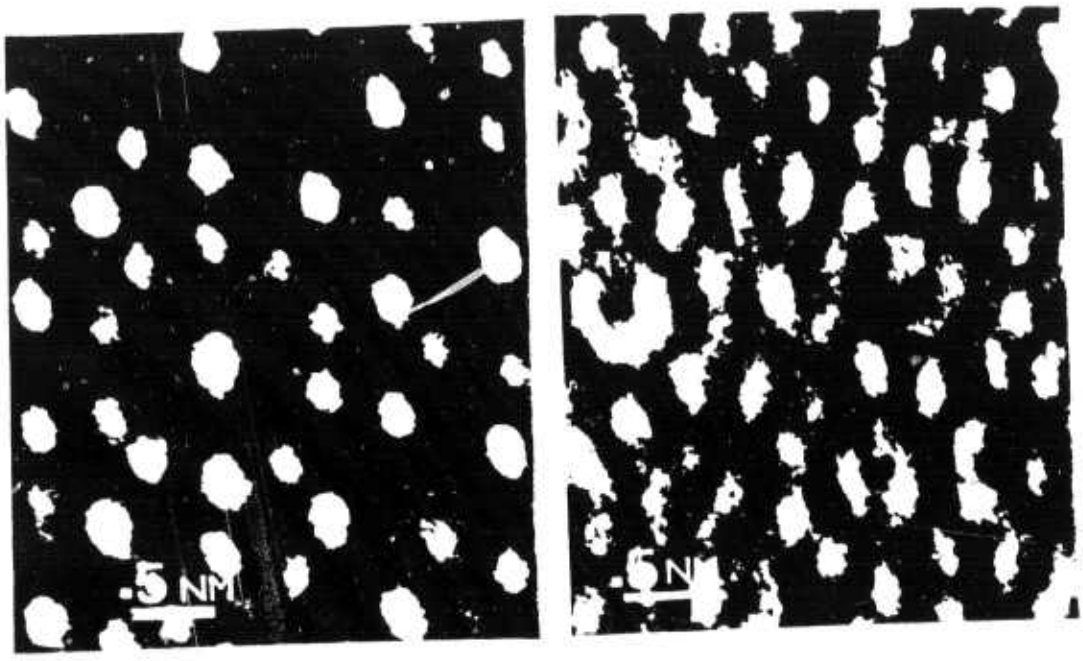

Figure 1: (a) 5-fold orientation at -90 Nm defocus with 0.08 Nm objective aperture. (b) -170Nm defocus, same aperture.

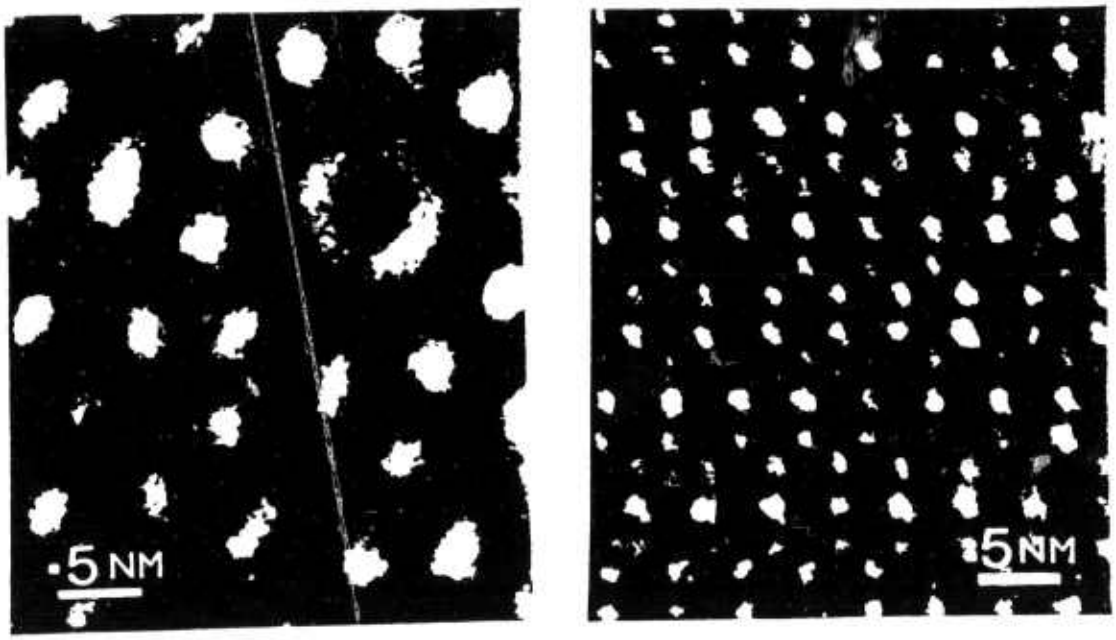

Figure 1: (c) 5-fold orientation at -150 Nm defocus with 0.03 Nm objective aperture.

Figure 2: 2-fold orientation at -50 Nm defocus with 0.05 Nm aperture.

Here too,the projected quasi-lattice nodes and intensity modulations of the images correspond: neither dynamical effects nor phase-changes due to aberrations can modify the intrinsic topology of the images. The unit length of the edge of the elementary rhombohedra (Mackay 1982, Kramer et al 1984) constituting the basic tiles for aperiodic space filling is .46 nm; this parameter gives a unit length of .65 nm for the 6-dimensionnal primitive hypercubic generating lattice. These values strongly suggest that the actual structure contains certainly more than one atom per unit cell; not only some of the Al-Mn distances in the usual crystalline phases are known to be abnormally short (Cooper et al 1966) but the intrinsic volumes of the rhombohedra are far too large to be consistent with the experimental density (Kelton et al 1985) if occupied by a single atom (an average of 4 atoms is expected). From the strict mathematical point of view, the C.P.M. is not able to make any distinction between any two homothetic quasi-lattices which are in the ratio τ^3 (where τ is the golden mean). This property is directly observed in both diffractions and images of the two-fold orientation /see Portier et al 1985 for a detailed discussion/ whereas an apparent τ scaling is observed on the five-fold orientation.

Convergent Beam Patterns of the different principal orientations all show an uniform contrast within the discs. This effect might be explained by the fact that the reciprocal quasi-lattice being a dense Z-modulus (see below), each intensity within the discs results from an infinite number of contributions of diffracted beams. An additional plausible explanation is the fact that actual quasi-crystals have a short correlation length (Bancel et al 1985) due to an imperfect quasi-periodicity in the material which would weaken the effect of the excitation parameters in the dynamical diffraction.

Discussion.

The very challenging problem which has to be solved is the description of the atomic structure. Electron microscopy is considered as being a suitable tool for collecting informations about the positions of the atoms and some models (Hiraga et al 1985, Guyot et al 1985, Knowles et al 1985) have already been proposed based mostly on only the five-fold orientation. There are, however, serious difficulties in interpreting the HR images: the dynamical calculations depend crucially on the number of allowed diffracted beams (Cornier et al this issue) which, contrary to the case of crystals, form a dense set. The so-called "small divisor" problem (Belissard 1982) in the almost periodic diffraction Hamiltonian makes the perturbation expansion diverge, leading to approximate solutions which are critically dependent on the chosen cut-off (Cornier et al this issue) . For an optimal cut-off, the simulated

dynamical images of a simple quasi-lattice with an average atom at each quasi-lattice node fit remarkably well the experimental ones (Cornier et al this issue). Hence, HR images of relatively close packed structures are essentially governed by the topology of the lattice and are quite insensitive to the atomic motif. Indeed, a specific result of the C.P.M. is that the Fourier components of the potential are multiplied by the Fourier transform of a generic cut function which does not depend on the atomic species. This term is so predominant that chemically different icosahedral phases -like those in Shechtman et al 1985 , Zhang et al 1985- do show very similar intensity distributions although they are constituted of different atoms. These reasons show that HR microscopy will be of limited use for the structure determination of metallic quasi-crystals.

References.

Bancel P.A., Heiney P.A., Stephens P.W., Goldman A.I. and Horn P.M. Phys Rev. Lett. 54, 2422 (1985)

Bellissard J. Lectures Notes in Phys. 153, 356 (1982) Springer Verlag

Besicovith A. "Almost periodic Functions", Cambridge ,1932

Cooper M. and Robinson K. Acta Cryst. 20, 614 (1966)

Cornier M.,Portier R. and Gratias D., this issue.

Duneau M. and Katz A. Phys. Rev. Lett. 54, 2688 (1985)

Elser V., Preprint to appear in Acta CrystA

Guyot P. and Audier M. Phil. Mag B, L15 (1985)

Hiraga K., Hirabayashi M., Inone A. and Masumoto A. Sc. Reports of the Res. Inst. Tohoku Univ. A32,2, 309 (1985)

Janssen T. and Janner A. Physica 126A, 163 (1984)

Kalugin P.A., Kitaev A.Y. and Levitov L.S. JETP Lett. 41, 145 (1985)

Kelton K.F. and Wu J.W. Appl. Phys. Lett. 46, 1059 (1985)

Knowles K.M., Greer A.L., Saxton W.O. and Stobbs W.M. Phil. Mag. B , L31 (1985)

Kramer P. and Neri R. Acta Cryst. A40, 580 (1984)

Levine D. and Steinhardt P.J. Phys. Rev. Lett. 53, 2477 (1985)

Mackay A.L. Physica 114A, 609 (1982)

Portier R., Shechtman D., Gratias D. and Cahn J.W. J. Mic. Spect. Elec. 10, 107 (1985)

Shechtman D., Gratias D. and Cahn J.W. C.R.A.S. 300 Serie II, 909 (1985)

Shechtman D., Blech I., Gratias D. and Cahn J.W., Phys. Rev. Lett. 53, 1951 (1984)

Zhang Z.,Yl H.Q. and Kuo K.H., Preprint to appear in Phil. Mag. B

Indexing of icosahedral quasiperiodic crystals

John W. Cahn
Institute for Materials Science and Engineering, National Bureau of Standards, Gaithersburg, Maryland 20899

Dan Shechtman[a)]
Department of Materials Engineering, Israel Institute of Technology, Technion, 32000 Haifa, Israel

Denis Gratias
C.E.C.M./C.N.R.S., 15 rue Georges Urbain, 94400 Vitry-sur-Seine, France

(Received 13 November 1985; accepted 10 December 1985)

Since the definition of quasiperiodicity is intimately connected to the indexing of a Fourier transform, for the case of an icosahedral solid, the step necessary to prove, using diffraction, that an object is quasiperiodic, is described. Various coordinate systems are discussed and reasons are given for choosing one aligned with a set of three orthogonal two-fold axes. Based on this coordinate system, the main crystallographic projections are presented and several analyzed single-crystal electron diffraction patterns are demonstrated. The extinction rules for three of the five icosahedral Bravais quasilattices are compared, and some simple relationships with the six-dimensional cut and projection crystallography are derived. This analysis leads to a simple application for indexing powder diffraction patterns.

I. INTRODUCTION

The recent discovery of Shechtmanite,[1,2] a metallic phase with long-range icosahedral orientational symmetry and experimentally discrete diffraction patterns, has revealed a new class of ordered structures. The icosahedral symmetry is inconsistent with strict crystallographic periodicity, yet discrete diffraction implies quasiperiodicity. Schechtmanite is thus cited as an example of a quasiperiodic crystal or quasicrystal, for short. Since the two icosahedral groups are not part of the 32 crystallographic point groups, the possibility exists that any of the infinity of noncrystallographic point groups will be observed. Indeed, claims that specimens exhibiting two other point groups, decagonal 10/m (Ref. 3) and duodecagonal 12 (Ref. 4), have since been reported.

These quasicrystalline phases present challenging problems in crystallography. In this paper the mundane housekeeping problems of coordinate systems, indexing, and extinction rules that are the essential language of reporting experimental observations will be discussed. Indexing is not just a housekeeping procedure: it is an essential part of proving that a structure is periodic, quasiperiodic, or almost periodic. We will concentrate on the icosahedral phases and the three-dimensional aspects of descriptions that are most easily derived in higher dimensions.

II. QUASIPERIODICITY

The Fourier transform of a periodic function is a set of delta functions that are periodically spaced and, in general, vary in magnitude. Diffraction gives information in the form of a Fourier transform of the correlations of an object. If the object is a periodic crystal, the diffraction pattern is a discrete set of spots of varying intensity that are positioned on a reciprocal lattice. Three reciprocal lattice vectors form a basis to locate any spot in a three-dimensional reciprocal space.

A mathematical function is quasiperiodic by definition if its Fourier transform is a set of delta functions that are not uniformly spaced as they would be for a periodic function, but whose spacing can be described by a finite set of lengths.[5] If an infinite number of lengths are required the function is called almost periodic. Therefore specimens that give countable diffraction spots that cannot be indexed with three reciprocal lattice vectors are quasiperiodic if they can be indexed with a finite set.

It has been shown that any D-dimensional quasiperiodic function requiring a basis of N vectors can be considered to be derived from a periodic N-dimensional function cut by a D-dimensional plane.[5] If every spot in the diffraction pattern can be indexed using a combination of N reciprocal lattice vectors, then the object that gave this diffraction pattern can be represented by a cut of a N-dimensional periodic object.

The icosahedral point group is not consistent with translational periodicity. The icosahedral diffraction pattern cannot consist of periodically spaced spots. If

[a)] Present address: Center for Materials Research, The Johns Hopkins University, Baltimore, MD 21218; also a guest worker at the National Bureau of Standards, Gaithersburg, MD 20899.

 0003-6951/86/010013-14$01.75

the diffraction pattern consists of discrete spots that can be indexed by a finite number of basis vectors it is quasiperiodic.

Several papers have already discussed ways of deriving quasiperiodic structures from cuts of periodic higher dimensional structures[6–10] including icosahedral structures. The converse problem of taking a particular diffraction pattern and indexing it has been attempted[11] in a way that has been criticized.[12,13] The problem centers on the fact that with a combination of incommensurate lengths any spot can be located approximately with any desired degree of accuracy. We will show that with our indexing, the observed high-intensity spots form a simple sequence in which none are missing and none left out.

III. COORDINATE SYSTEMS

Taking basis vectors along important symmetry directions simplifies the crystallographic formulation. For any group with a unique rotation axis, the z axis is taken parallel to that axis. This is the proper choice for the crystallographic groups such as hexagonal and the noncrystallographic groups such as decagonal. The icosahedral groups have 6 fivefold axes, 10 threefold axes, and 15 twofold axes. Taking one of the fivefold axes as the z axis (Fig. 1) leaves the other five in a ring 63.43° from this axis. Although these all would make acute angles with the z axis, there are obtuse angles between some of them. There is no choice of sign for the six axes that would give equal angles between all of them. A co-

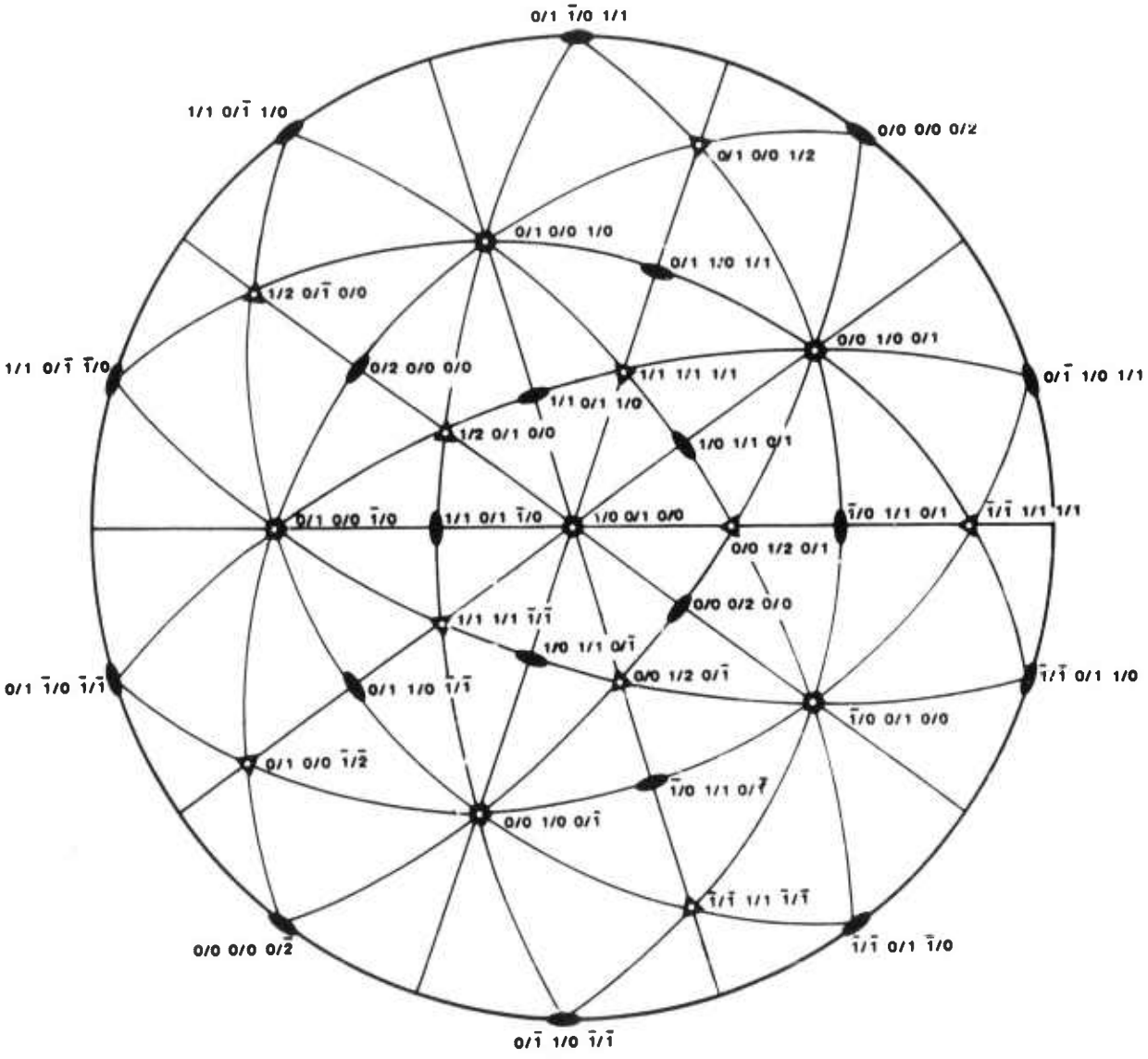

FIG. 1. The stereographic projection of the principal symmetry directions and mirror planes of the icosahedral group $m\bar{3}\bar{5}$ as seen along the fivefold direction. The number indicates the indexing system that will be described later in the text.

ordinate system based on these axes is not only skewed but encounters the difficulty of keeping track of obtuse and acute angles. There are right angles between a fivefold axis and five of the twofold axes, that could serve as a coordinate system when comparing the icosahedral phase with the decagonal phase.

If we examine the icosahedral group with a threefold axis along z (Fig. 2), we have three choices of coordinate systems that are related to familiar crystallographic ones. The 6 fivefold axes now fall into two groups, either of which could be used as a rhombohedral basis. In one set the fivefold axes make acute angles with each other. In the other set the angles are obtuse. A hexagonal coordinate system could be based on the threefold axis and the three twofold axes at right angles to it. Of special interest are the three twofold axes at 71° from z that form an orthogonal set.

The simplest system is a cubic coordinate system in which the axes of the coordinate system are aligned with a set of three orthogonal twofold axes of the icosahedral group (Fig. 3). The 15 twofold axes fall in five such sets all equivalent to each other through the operation of a fivefold axis. This is the coordinate system used in the International Tables of Crystallography, and it is the coordinate system we will use, even to describe the other coordinate systems. It has all advantages of orthogonal axes.

The three coordinate systems discussed here are all based on subgroups of the icosahedral group, as shown in Fig. 4. Using a coordinate system based on a lower symmetry than icosahedral, requires special attention for the icosahedral symmetries not used in that coordinate system: equivalent reflections will not necessarily have similar indices.

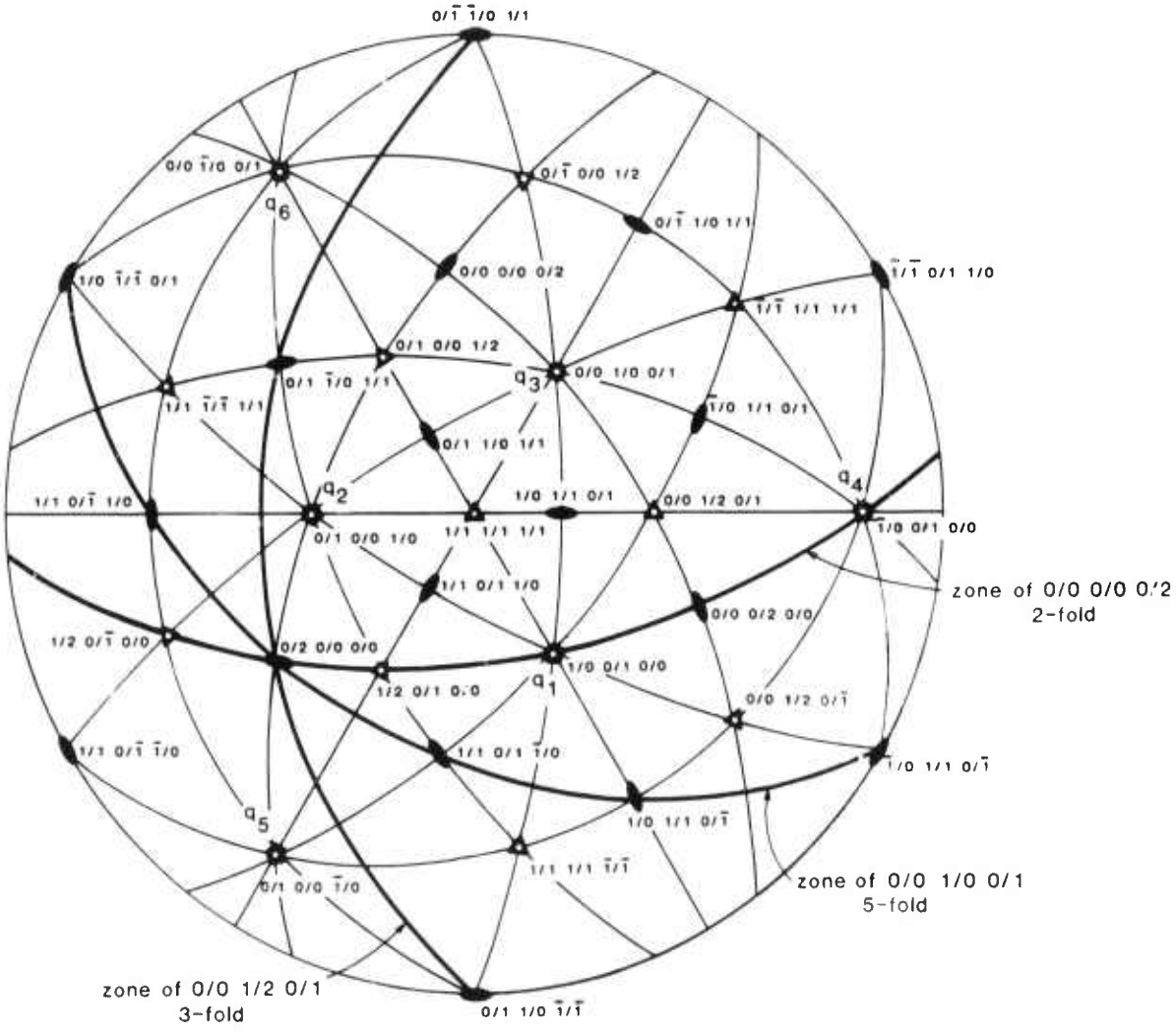

FIG. 2. The stereographic projection of the icosahedral group $m35$ as seen along a threefold direction. Note the possibility of a rhombohedral coordinate system using either set of fivefold axes, a hexagonal coordinate system using the twofold axes along the equator or the three twofold axes at 71°. The thickened great circles show the three zone axes of the diffraction pattern indexed in Figs. 5–7, namely the twofold labeled [0/0 1/0 0/1], the fivefold labeled [0/0 1/0 0/1] and the threefold axis labeled [0/0 1/2 0/1].

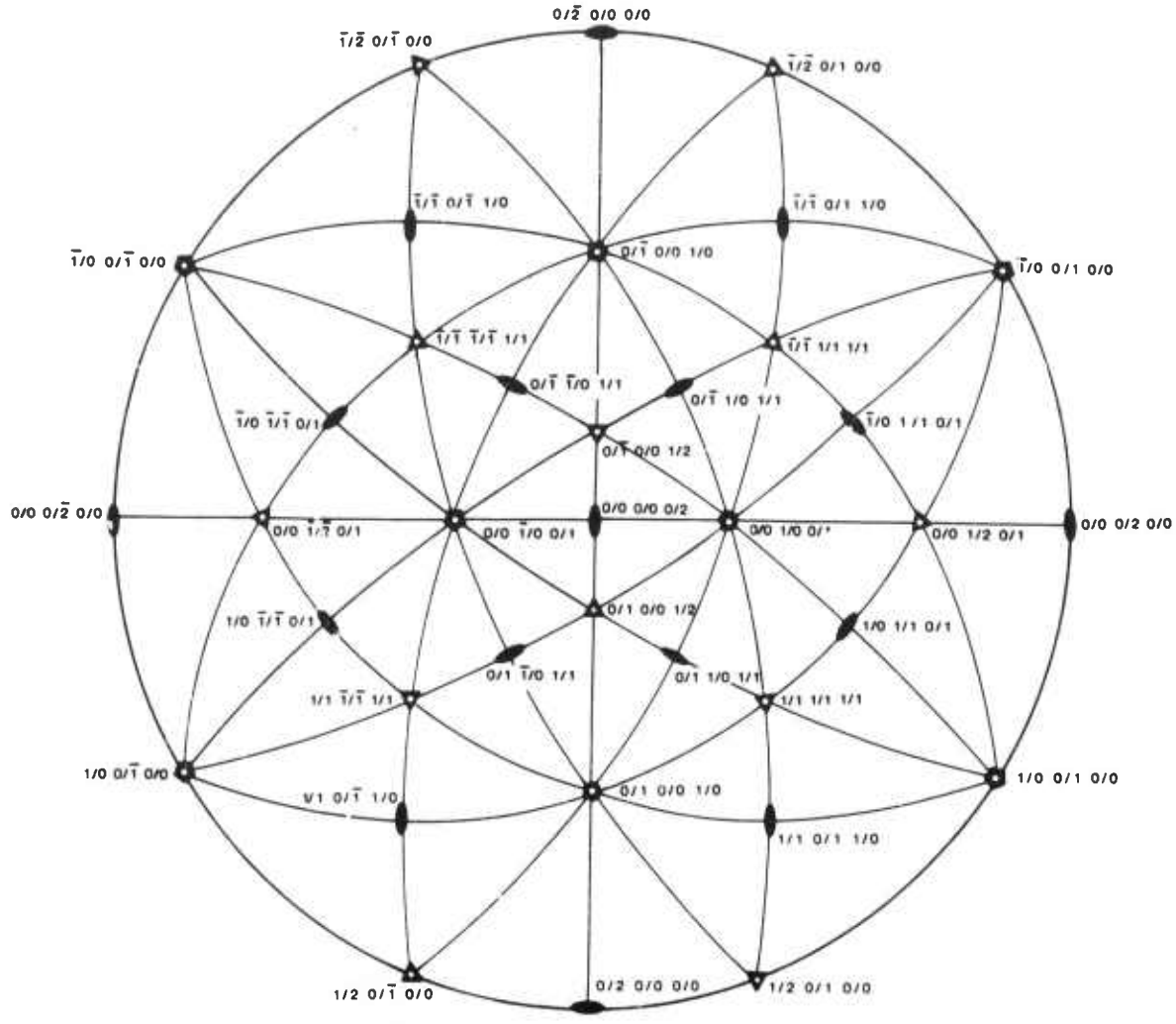

FIG. 3. The standard stereographic projection for the icosahedral group aligns the axes of an orthogonal coordinate system with one of the five sets of mutually perpendicular twofold axes. Note that four of the threefold axes are along the ⟨111⟩ directions.

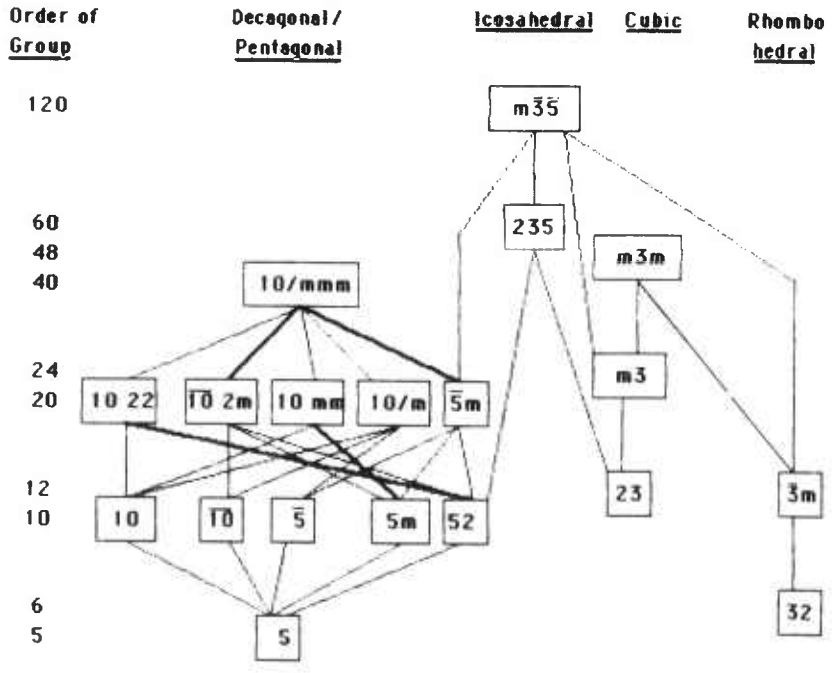

FIG. 4. The maximal subgroups of the icosahedral group $m\bar{3}\bar{5}$ and the decagonal group $10/mmm$.

IV. THE CUBIC COORDINATE SYSTEM

Having selected a coordinate system aligned along three perpendicular twofold axes, we need to describe vectors and planes in both the direct and reciprocal spaces. An immediate advantage of the choice of a cubic coordinate system is that the indices of a plane and the direction normal to it are the same. We define unit lengths a and a^* in both spaces and dimensionless lengths and position in terms of these. Consider a position (UVW) or a plane (HKL). The set of all positions or planes equivalent through the operations of the icosahedral groups (235) and $m\bar{3}\bar{5}$ is as follows:

1. The threefold axes give cyclic permutation, but note that while (UVW), (WUV), and (VWU) are equivalent, (VUW), etc., is different.

2. The twofold axes give pairs of sign changes, the mirrors give individual sign changes. Thus for 235, (UVW), $(\bar{U}\bar{V}W)$, $(U\bar{V}\bar{W})$, and $(\bar{U}V\bar{W})$ are equivalent but $(\bar{U}\bar{V}\bar{W})$, etc., is not. For $m\bar{3}\bar{5}$ all sign changes are equivalent positions.

3. The fivefold axes introduce a change of the magnitude of U, V, and W and introduce the golden section $\tau = 2\cos 36^\circ = (1+\sqrt{5})/2 = 1.618\,034$. Because the International Tables have a misprint in the rotation matrices, we repeat them here in Table I, using their notation $G = \tau/2, g = 1/2\tau = G - 1/2$. Performing the matrix multiplication we obtain

$$\begin{aligned}(HKL)Y &= \tfrac{1}{2}[(H-K)+\tau(K-L),\\ &\quad (L-H)+\tau(H+K),\\ &\quad -(K+L)+\tau(L+H)].\end{aligned} \tag{1}$$

In this multiplication we make frequent use of the identities

$$\tau^2 = 1+\tau, \tag{2}$$

$$1/\tau = \tau - 1, \tag{3}$$

$$G^2 + g^2 + (\tfrac{1}{2})^2 = 1. \tag{4}$$

It may at first seem surprising that equivalent positions turn out to have designations with different numerical values of the components, but this is unavoidable with a Cartesian coordinate system and groups with such a high symmetry. The most symmetric crystallographic group $m\bar{3}m$ has order 48. It has 48 unit triangles. Taking all the permutations and sign changes of (UVW) generates 48 equivalent general positions, one in each unit triangle. It is impossible to generate the 60 or 120 equivalent positions needed (resp. for 235 or $m\bar{3}\bar{5}$) with just three symbols. Thus, the choice of a cubic coordinate system results in the possibility that as many as five different sets of indices may be necessary to represent equivalent positions or planes.

Now consider a plane or reciprocal space position with an index of the form

$$(h+h'\tau, k+k'\tau, l+l'\tau),$$

that is, where

$$H = h+h'\tau, \quad K = k+k'\tau, \quad L = l+l'\tau,$$

in which the h, h', k, k', l, and l' are all integers. We introduce the six-index notation $(h/h', k/k', l/l')$ or $(h/h'\ k/k'\ l/l')$ to designate such a reflection.

Operation of the fivefold rotation will change the numerical value of the six integers.

$$\begin{aligned}&(h+h'\tau, k+k'\tau, l+l'\tau)Y\\ &\quad = \tfrac{1}{2}[(h+k')-(k+l')\\ &\qquad +\tau[(-l+h')+(k-l')],\\ &\quad (-h+k')+(l+h')\\ &\qquad +\tau[(h+k')+(k+l')],\\ &\quad (-k+l')+(l+h')\\ &\qquad +\tau[(h-k')+(l+h')]].\end{aligned} \tag{5}$$

In order for this to be a close set, we impose the parity conditions that the three sums $h+k'$, $k+l'$, and $l+h'$ are even: after fivefold rotation the six integer indices remain integers and the parity rules are conserved.

TABLE I. Matrices for fivefold rotation about $[1\ \tau\ 0]$.

$$Y = Y^{-4} = \begin{pmatrix} \tfrac{1}{2} & g & G \\ g & G & -\tfrac{1}{2} \\ G & \tfrac{1}{2} & g \end{pmatrix} \qquad Y^2 = Y^{-3} = \begin{pmatrix} -g & G & \tfrac{1}{2} \\ G & \tfrac{1}{2} & -g \\ -\tfrac{1}{2} & g & -G \end{pmatrix}$$

$$Y^3 = Y^{-2} = \begin{pmatrix} -g & G & -\tfrac{1}{2} \\ G & \tfrac{1}{2} & g \\ \tfrac{1}{2} & -g & -G \end{pmatrix} \qquad Y^4 = Y^{-1} = \begin{pmatrix} \tfrac{1}{2} & g & -G \\ g & G & \tfrac{1}{2} \\ G & -\tfrac{1}{2} & g \end{pmatrix}$$

$G = (\sqrt{5}+1)/4 = \tau/2 = \cos 36^\circ = 0.809017$

$g = (\sqrt{5}-1)/4 = 1/2\tau = G - \tfrac{1}{2} = \cos 72^\circ = 0.309017$

$Y^T = Y^{-1}$

Finding that all spots in the diffraction pattern are of this form implies quasiperiodicity.

We next turn to the indexing of the principal directions (Figs. 1–3). The six fivefold axes are all of the form $(1\tau 0)$, or in the six-index notation (1/0 0/1 0/0).

The ten threefold axes have two different designations: four are along (111) or (1/0 1/0 1/0) and six along $(\tau^2\ 1\ 0)$ or (1/1 1/0 0/0). Note that both vectors have been chosen to have a length $\sqrt{3}$.

Three of the twofold axes are along the cube axes. The remaining 12 have the form $(G, g, \frac{1}{2})$ or $(0/1\ \bar{1}/1\ 1/0)$.

V. RECIPROCAL QUASILATTICES

Consider a quasilattice in three-dimensional reciprocal space in which every spot occurs as a sum of integer multiples of a finite number (greater than three) of vectors. We will compare two lattices formed only of equivalent vectors. In particular, let us first take the six vectors along the fivefold axes,[14]

$$\mathbf{Q} = \sum_{i=1}^{6} n_i \mathbf{q}_i, \tag{6}$$

where the n_i are integers and the $\mathbf{q}_i$ are $(1\tau 0)$ which in the six-index notation is

$$\begin{aligned}
\mathbf{q}_1 &= (1/0\ 0/1\ 0/0),\\
\mathbf{q}_2 &= (0/1\ 0/0\ 1/0),\\
\mathbf{q}_3 &= (0/0\ 1/0\ 0/1),\\
\mathbf{q}_4 &= (\bar{1}/0\ 0/1\ 0/0),\\
\mathbf{q}_5 &= (0/1\ 0/0\ \bar{1}/0),\\
\mathbf{q}_6 &= (0/0\ \bar{1}/0\ 0/1).
\end{aligned} \tag{7}$$

[There are 384 ways for choosing the q_i's. All give equivalent results. The choice of the set (7) corresponds to the two rhombohedral bases: $\mathbf{q}_1$, $\mathbf{q}_2$, $\mathbf{q}_3$ define the acute rhombohedron and $\mathbf{q}_4$, $\mathbf{q}_5$, $\mathbf{q}_6$ the obtuse one (see Fig. 2).] The set of six numbers (n_i) can be considered an indexing of Q, and has been used in a number of papers. This same set can also be considered to be a six-dimensional lattice vector. To express Q in terms of the three-dimensional cubic coordinates we substitute set (7) in Eq. (6) and perform the summation,

$$\begin{aligned}
Q = [&(n_1 - n_4)/(n_2 + n_5),\ (n_3 - n_6)/(n_1 + n_4),\\
&(n_2 - n_5)/(n_3 + n_6)].
\end{aligned} \tag{8}$$

We can thus convert from the six-dimensional vector $(n_1, n_2, n_3, n_4, n_5, n_6)$ to the six-index three-dimensional vector $(h/h', k/k', l/l')$.

$$\begin{aligned}
h &= n_1 - n_4, \quad h' = n_2 + n_5,\\
k &= n_3 - n_6, \quad k' = n_1 + n_4,\\
l &= n_2 - n_5, \quad l' = n_3 + n_6,
\end{aligned} \tag{9a}$$

and vice versa

$$\begin{aligned}
2n_1 &= h + k', \quad 2n_4 = -h + k',\\
2n_2 &= l + h', \quad 2n_5 = -l + h',\\
2n_3 &= k + l', \quad 2n_6 = -k + l'.
\end{aligned} \tag{9b}$$

The form of Eq. (9b) demonstrates that Q in the six-index notation obeys the parity rules. These restrictions on the indices are extinction rules and are given in Table II under the heading of the P quasilattice (to be defined later).

These parity rules lead to four kinds of positions:

1. six even indices,
2. four even indices (odd/even, even/odd, even/even),
3. two even indices (even/odd, odd/even, odd/odd),
4. six odd indices.

If the coordinates of a spot (HKL) that is consistent with the parity rules are multiplied by τ, the results are

$$\begin{aligned}
(\tau H\ \tau K\ \tau L) = [&h'/(h + h'), k/(k + k'),\\
&l'/(l + l')].
\end{aligned} \tag{10}$$

Only if the original $(HKL) = (h/h'\ \ k/k'\ \ l/l')$ contains two or six even indices, will $(\tau H\ \tau K\ \tau L)$ satisfy the parity rules. On the other hand, scaling by τ^3

$$\begin{aligned}
(\tau^3 H\ \tau^3 K\ \tau^3 L) = [&(h + 2h')/(2h + 3h'),\\
&(k + 2k')/(2k + 3k'),\\
&(l + 2l')/(2l + 3l')]
\end{aligned} \tag{11}$$

preserves the parity rules for all (HKL) that satisfy them. These scaling rules are tabulated for the primitive (P) reciprocal quasilattice in Table III.

In addition, the square of Q is of the form

$$Q^2 = N + M\tau, \tag{12}$$

where using Eqs. (2) and (3),

TABLE II. Extinction rules for reciprocal quasilattices.

	$P(a^*)$	$F(2a^*)$ direct lattice is $I(a)$	$I(2a^*)$ direct lattice is $F(a)$
HKL	$h + k' = 2n$ $k + l' = 2n$ $l + h' = 2n$	same as P^* plus $h + k + l = 2n$ $(h' + k' + l' = 2n)$	all even plus $h + l + h' + k' = 4n$ $h + k + l' + k' = 4n$ $(l + k + h' + l' = 4n)$
n_i	all integers	$\Sigma n_i = 2n$	all even or all odd

TABLE III. Parity and scaling properties for the P and F reciprocal quasilattices.

Parity of indexes	Scaling	P	F	$Q^2 = N + \tau M$ N	M
six even	τ	Present	Present	$4n$	$4m$
four even	τ^3	Present	Absent	$4n+2$	$4m+1$
two even	τ	Present	Present	$4n$	$4m$
six odd	τ^3	Present	Absent	$4n+2$	$4m+1$

$$N = 2\sum_{i=1}^{6} n_i^2 = h^2 + h'^2 + k^2 + k'^2 + l^2 + l'^2, \quad (13)$$

$$M = h'^2 + k'^2 + l'^2 + 2(hh' + kk' + ll'). \quad (14)$$

Equation (13) indicates that N, the integer part of Q^2, is twice the square of the length of the six-dimensional n vector and therefore must be even. Because of the parity rules, if N is divisible by 4, M also is divisible by 4, and if N is not divisible by 4, M is of the form $4m+1$. In addition, as we will show later, M conforms to the limits

$$-N/\tau < M < N\tau \quad (15)$$

and that the most intense reflections occur for the largest value of M, which we shall denote by M_0. For N divisible by 4

$$M_0 = 4\,\lfloor (N\tau)/4 \rfloor, \quad (16)$$

where $\lfloor x \rfloor$ is the largest integer in x.
When N is not divisible by 4,

$$M = 4m + 1 < N\tau.$$

The largest value of the integer m is

$$m_0 = \lfloor (N\tau - 1)/4 \rfloor$$

and

$$M_0 = 1 + 4\,\lfloor (N\tau - 1)/4 \rfloor. \quad (17)$$

We next define a two-parameter indexing $Q(N,r)$

$$Q^2(N,r) = N + M_0\tau - 4r\tau,$$
$$r = 0,1,\ldots < \lfloor (N/\tau + M_0)/4 \rfloor, \quad (18)$$

in which the $Q_0(N)$ will turn out to define the sequence of intense reflections.

$$Q_0^2(N) = Q^2(N,0) = N + M_0(N)\tau. \quad (19)$$

The same procedure has been used by us to find the quasilattice formed from the 15 vectors along the twofold axes. The same result is obtained in a similar manner by putting the face-centering restrictions F on the six-dimensional lattice formed by the n_i, and then using Eq. (9a). The result for that and for the body-centered I lattice are also given in Table II.

In Table III we make a simple comparison between the P and F which share the same parity rules. It can be seen that the F lattice scales by τ, and has only $N = 4n$, the P lattice comprises, in addition, $N = 4n+2$ spots that scale by τ^3. Figure 5 is a diffraction intensity calculation using the sphere approximation in the cut and projection method.[8,9]

VI. INDEXING THE SINGLE QUASICRYSTAL PATTERNS

Figures 6–8 show the indexing of the electron diffraction patterns of Refs. 1 and 2. The stereographic projection (Fig. 2) presents the three zone axes of these diffraction patterns, namely, the [0/0 0/0 0/2] twofold, the [0/0 1/0 0/1] fivefold, and the [0/0 1/2 0/1] threefold axes. Note that all of the reflections in the fivefold and threefold zone axis conform to either the P or F reciprocal quasilattices of Sec. V. These could not be used to distinguish between the two reciprocal quasilattices.

It is easy to show that the reflections for which $h' + k' + l'$ is odd will appear in neither the five- or

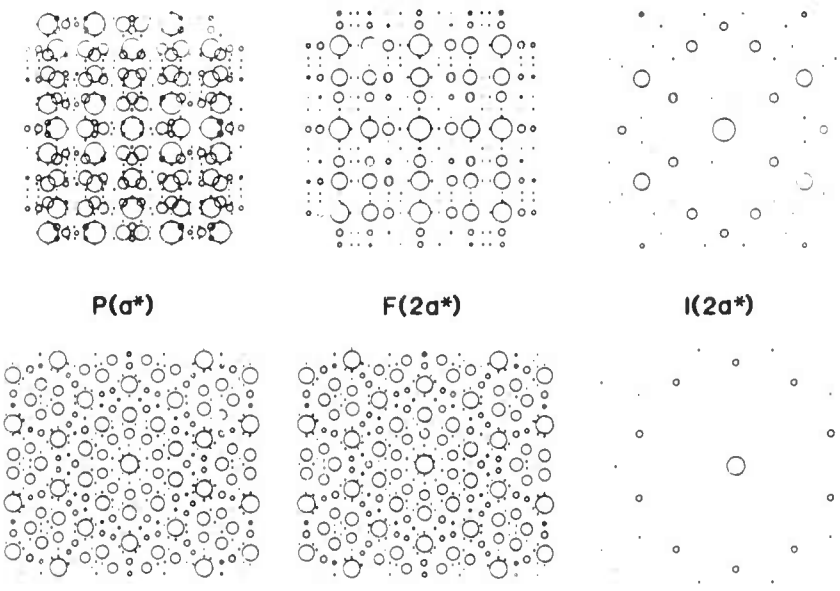

FIG. 5. Diffraction patterns calculated by the cut and projection method for all three reciprocal cubic quasilattices with the same lattice parameter a^* for the two- and fivefold zone axes.

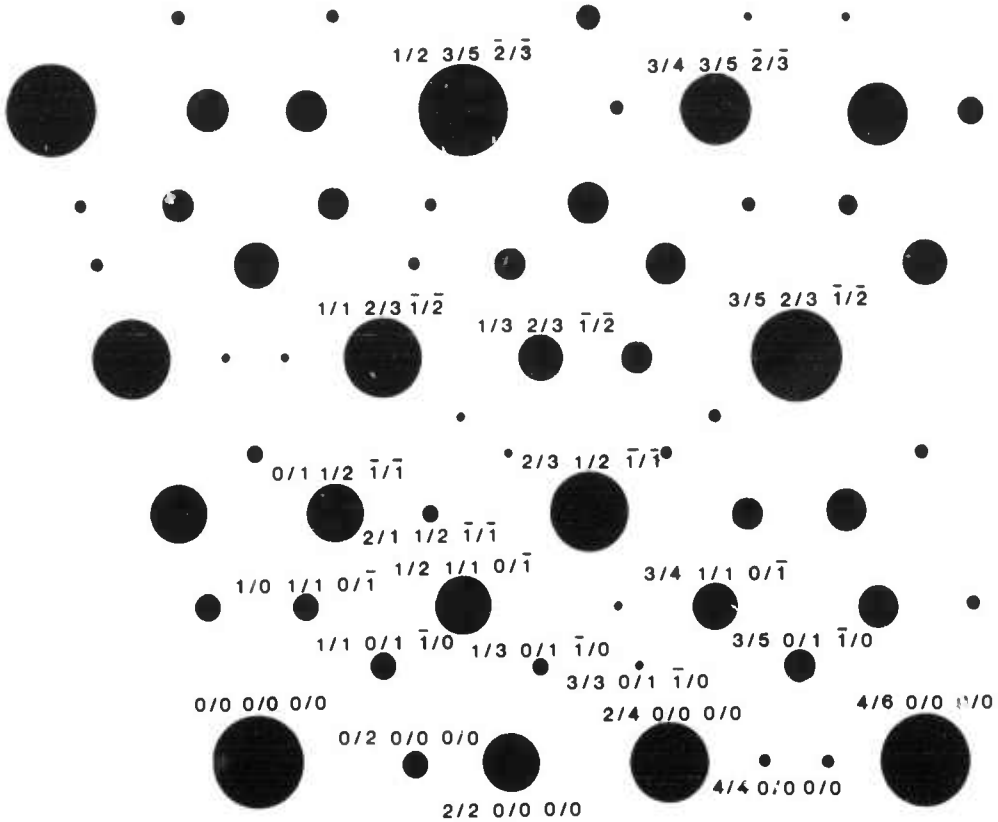

FIG. 6. Indexed diffraction pattern of a 108° sector of the [0/0 1/0 0/1] zone axis. Sizes of the circles represent calculated intensities based on the inverse of the distance of a spot in the six-dimensional primitive reciprocal lattice from the cut plane.

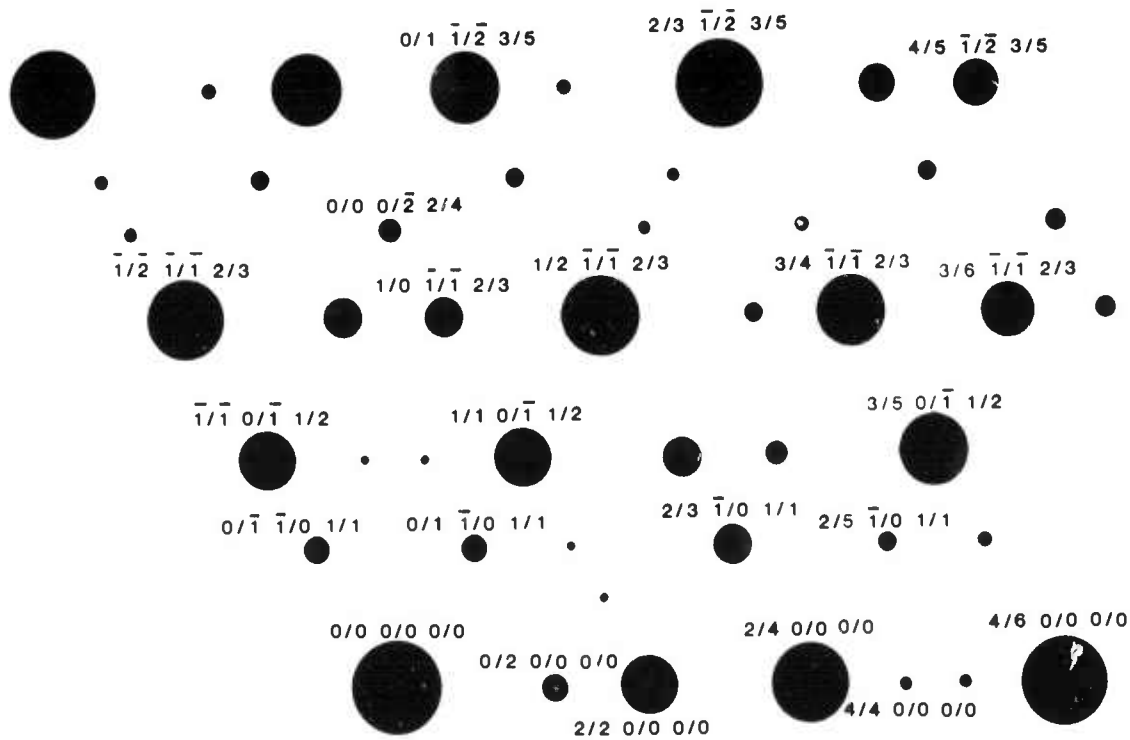

FIG. 7. Indexed diffraction pattern of a 120° sector of the [0/0 1/2 0/1] zone axis.

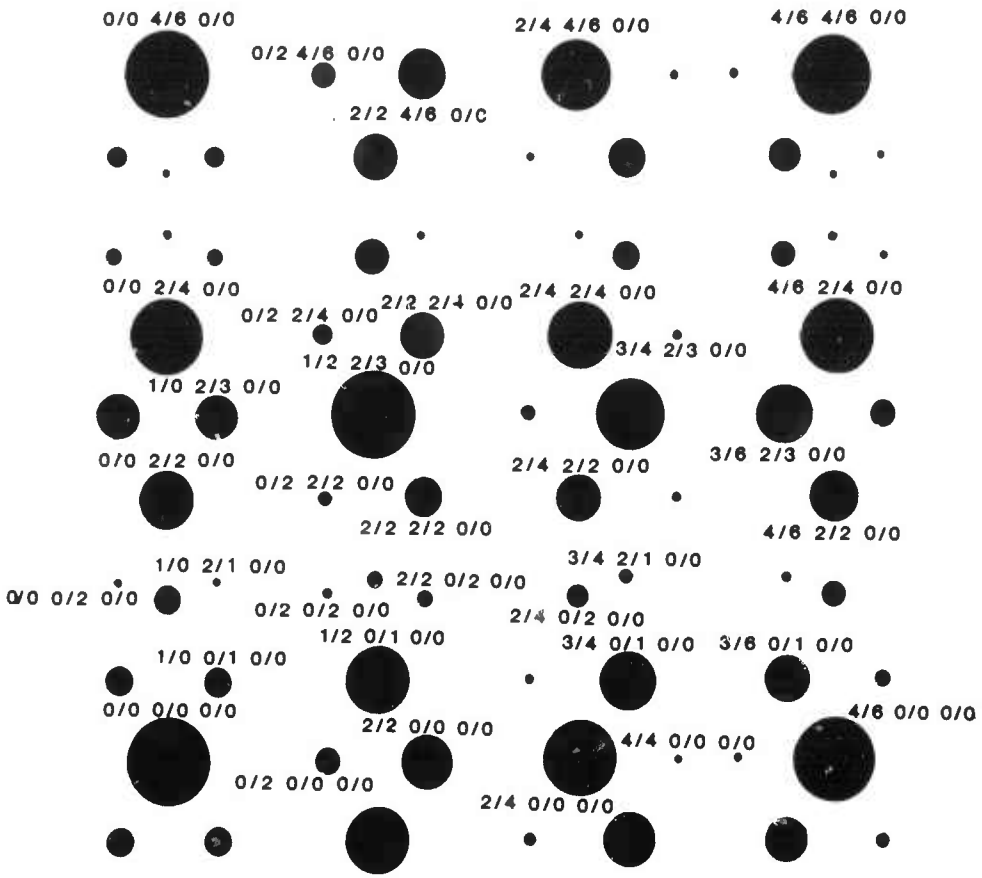

FIG. 8. Indexed diffraction pattern of the [0/0 0/0 0/2] zone axis. Note the square array made of all even and two-even spots that scale with τ. If only these spots were present, this pattern would have fourfold symmetry and scale by τ.

threefold zone axes. For example, in order for a reflection to be in the [0/0 1/0 0/1] zone axis $K + \tau L = 0$. This implies that $k + l' + \tau(k' + l + l') = 0$, which can only occur if $(k + l') = (k' + l + l') = 0$. Adding the even number $h' - l$ gives $h' + k' + l' = 2n$. The same result is obtained with the [111] zone axis. Fitting the two zone axes alone can not distinguish between P and F. Indeed the model of Levine and Steinhardt seems to fit only the three- or fivefold.[14] In the [0/0 0/0 0/2] zone axes $l = l' = 0$, but $h + k$ (and $h' + k'$) can be odd. This gives the spots with two odd indices, that can be seen in Fig. 7. Spots with six odd indices derive from these after some fivefold rotations. The twofold zone axes thus show some spots with τ^3 scaling.

The twofold zone axis for the F quasilattice show only spots with τ scaling and may show an accidental fourfold symmetry. Permutation of the x and y indices preserves the parity rules and does not change Q_c (see Sec. VII). If the intensity is only a function of Q_c the pattern will show the fourfold axis.

Observing an icosahedral diffraction pattern in which all the spots can be indexed with this six index notation proves that we have a diffraction pattern of a quasiperiodic structure. In particular the experimental pattern is not the F or I. Furthermore, because it can be indexed with six integers, the object can be represented as a slice and projection of a six-dimensional periodic structure.

Several other methods of indexing with six numbers have been successful.[11–13] They have differed from each other in ways that become significant after we examine the cut and projection method.

VII. THE CUT AND PROJECTION FROM SIX DIMENSIONS

In three dimensions the six vectors along the fivefold axes are not orthogonal. We can choose the six-dimensional cubic space in which each of these vectors is a basis vector along a hypercube axis that is perpendicular to all the others. The set of the six numbers n_i then represents a position vector in the six-dimensional cubic reciprocal lattice, and the equations (8) give the correspondence between positions in the three- and six-dimensional spaces. The cut and projection is accomplished by rotating the six-dimensional space so that what will become three axes in the three-dimensional space are in the cut plane. The six-dimensional rotation matrix corresponding to the chosen set (7) is

$$R = \frac{1}{\sqrt{2(2+\tau)}} \times \begin{bmatrix} 1 & \tau & 0 & -1 & \tau & 0 \\ \tau & 0 & 1 & \tau & 0 & -1 \\ 0 & 1 & \tau & 0 & -1 & \tau \\ -\tau & 1 & 0 & \tau & 1 & 0 \\ 1 & 0 & -\tau & 1 & 0 & \tau \\ 0 & -\tau & 1 & 0 & 1 & \tau \end{bmatrix} \quad (20)$$

The three-by-six matrix constituting the top half of the rotation matrix consists of the six fivefold directions in three dimensions as column vectors [compare with Eq. (7)], or the coordinates of the three-dimensional cube axes in the six-dimensional space as row vectors. The bottom three by six matrix consists of the complementary orthogonal space lost by the cut. It consists of projection directions from six dimensions into the real space. In the six-dimensional reciprocal space the distance of a spot from the cut plane is related to its intensity in the three-dimensional reciprocal space.

There are five Bravais lattices consistent with icosahedral symmetry in six dimensions.[10] Three of these are the P, I, F hypercubic. Consider first the primitive lattice. Its reciprocal lattice is also primitive. Because the projection of each six-dimensional lattice vector is a (1/0 0/1 0/0) vector along the fivefold axes, the reciprocal quasilattice observed experimentally to be one composed of such vectors will be denoted P. The other lattices in our example correspond to the six-dimensional face-centered F and body-centered I reciprocal lattices F corresponding resp. to I and F direct lattices.

In the P six-dimensional lattice the location of a spot in the dimensionless units that we have used in three dimensions is, using Eq. (20):

$$\mathbf{Q}_6 = \sqrt{2(1+\tau^2)}\,(n_1, n_2, n_3, n_4, n_5, n_6). \quad (21)$$

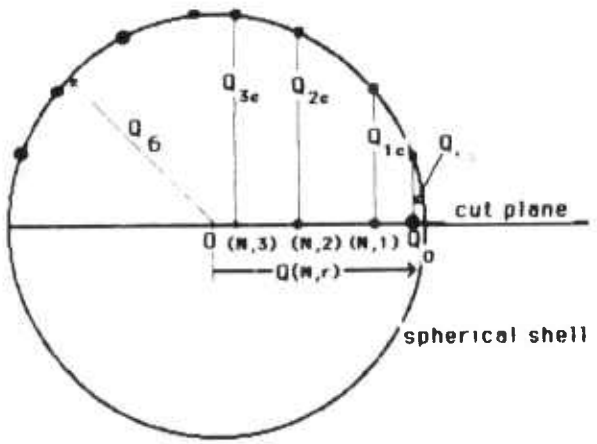

FIG. 9. Two-dimensional representation of the cut and projection procedure for the magnitude of Q and the distance from the cut plane Q_c.

As a result, using Eqs. (2) and (13),

$$Q_6^2 = 2(2+\tau)(n_1^2 + n_2^2 + n_3^2 + n_4^2 + n_5^2 + n_6^2) = (2+\tau)N. \quad (22)$$

The length of Q_6 is related to the N part of the length of Q (Fig. 9). Since projection shortens Q

$$Q^2 < Q_6^2. \quad (23)$$

Using Eqs. (12) and (22)

$$N + M\tau < (2+\tau)N.$$

Therefore

$$M < [(1+\tau)/\tau]N = \tau N. \quad (24)$$

Since $Q^2 > 0$, we also have

$$-N/\tau < M \quad (25)$$

proving the inequality (15). If we define Q_c to be the distance of a spot in the six-dimensional reciprocal space from the cut plane (Fig. 8), we have

$$Q_c^2 = Q_5^2 - Q^2 = \tau(N\tau - M). \quad (26)$$

Thus the largest M for a given N will have the smallest Q_c.

Up to now we have been using a dimensionless Q. We introduce a three-dimensional quasilattice constant d_0 such that the three-dimensional diffraction vector k and the interplanar spacing are given by

$$\mathbf{k} = \mathbf{Q}/d_0, \quad (27)$$

$$d(h/h', k/k', l/l') = d_0/\sqrt{N + \tau M}. \quad (28)$$

The length of the six-dimensional reciprocal lattice constant a_6^* is related to d_0 by

$$a_6^* d_0 = \sqrt{2(2+\tau)}. \quad (29)$$

In Table IV we give the values of $Q_0(N)$ and the corresponding Q_c that according to theory should be inversely correlated with intensity. This sequence of Q's has an obvious beginning ($N = 2$) and using $d_0 = 1.7466$ nm we produce for 0.155 nm radiation two further columns, the diffraction vector **k** and the diffraction angle 2θ. Comparing these with our own and published powder diffraction data[11] indicates a one-to-one correspondence with this list. The only omissions are due to overlap with fcc aluminum and low intensities in the published data.[11] The justification for our choice of d_0 is to match Table IV with experimental data. The choice of d_0 in Ref. 11 was different and this leads to complications to be discussed.

In Table V we list the $Q_0(N)$ series in three different notations each using six indices. The (n_i) and $(h/h'\,k/k'\,l/l')$ are representative of that particular $Q_0(N)$. The six-dimension (n_i) vector is that which projects into the longest possible three-dimensional vec-

TABLE IV. Scattering variables for the P lattice.

	Dimensionless			Dimensional ($d_0 = 1.74657$)	
N	M_0	Q_0^2	Q_c	$d^{-1}(\mathrm{nm}^{-1})$	2θ
2	1	3.62	1.90	1.089	9.68
4	4	10.47	2.00	1.853	16.51
6	9	20.56	1.07	2.596	23.21
8	12	27.42	1.24	2.998	26.87
10	13	31.03	2.27	3.189	28.62
12	16	37.89	2.35	3.524	31.70
14	21	47.98	1.64	3.966	35.80
16	24	54.83	1.75	4.239	38.36
18	29	64.92	0.45	4.613	41.90
20	32	71.78	0.76	4.850	44.16
22	33	75.40	2.05	4.971	45.32
24	36	82.25	2.14	5.192	47.46
26	41	92.34	1.32	5.502	50.48
28	44	99.19	1.45	5.702	52.45
30	45	102.81	2.39	5.805	53.47
32	48	109.67	2.47	5.996	55.38
34	53	119.76	1.80	6.265	58.10
36	56	126.61	1.91	6.442	59.90
38	61	136.70	0.89	6.694	62.50
40	64	143.55	1.08	6.860	64.23
42	65	147.17	2.19	6.946	65.13
44	68	154.03	2.27	7.105	66.83
46	73	164.12	1.52	7.334	69.28
48	76	170.97	1.64	7.486	70.93
50	77	174.59	2.51	7.565	71.79
52	84	187.91	0.47	7.848	74.92
54	85	191.53	1.96	7.923	75.77
56	88	198.39	2.05	8.064	77.36
58	93	208.48	1.17	8.267	79.68
60	96	215.33	1.32	8.401	81.25
62	97	218.95	2.32	8.472	82.07
64	100	225.80	2.40	8.603	83.63
66	105	235.89	1.70	8.793	85.92
68	108	242.75	1.81	8.920	87.47
70	113	252.84	0.65	9.104	89.74
72	116	259.69	0.90	9.226	91.29
74	117	263.31	2.10	9.290	92.11
76	120	270.16	2.19	9.410	93.66
78	125	280.25	1.40	9.584	95.94
80	128	287.11	1.53	9.701	97.50
82	129	290.73	2.44	9.762	98.32
84	132	297.58	2.52	9.876	99.89
86	137	307.67	1.87	10.042	102.21
88	140	314.52	1.97	10.154	103.79
90	145	324.61	1.00	10.315	106.15
92	148	331.47	1.18	10.424	107.77
94	149	333.09	2.24	10.480	108.63
96	152	341.94	2.32	10.587	110.27
98	157	352.03	1.59	10.742	112.71
100	160	358.89	1.71	10.846	114.40
102	165	368.98	0.25	10.997	116.93

TABLE V. Various indexing methods for the first 12 strong reflections.

N	M_0	(n_i)	$(h/h'\,k/k'\,l/l')$	multiplicity	Ref. 11
2	1	(100000)	(1/0 0/1 0/0)	12	$(21\bar{1}\bar{1}\bar{1}\bar{1})$
4	4	(100100)	(0/0 0/2 0/0)	30	$(2200\bar{1}\bar{1})$
6	9	(111000)	(1/1 1/1 1/1)	20	(110001)
					$(32\bar{1}\bar{1}\bar{1}2)$
8	12	$(10110\bar{1})$	(0/0 2/2 0/0)	30	$(1110\bar{1}0)$
10	13	$(11101\bar{1})$	(1/2 2/1 0/0)	60	$(2210\bar{2}0)$
12	16	(210010)	(2/2 0/2 0/0)	60	$(31\bar{1}\bar{1}\bar{1}\bar{1})$
		$(11111\bar{1})$	0/2 2/2 0/0)	12	
14	21	$(20110\bar{1})$	(1/0 2/3 0/0)	60	$(21\bar{1}001)$
					$(3310\bar{2}1)$
16	24	$(21101\bar{1})$	(2/2 2/2 0/0)	60	$(21\bar{1}\bar{1}01)$
18	29	$(21111\bar{1})$	(1/2 2/3 0/0)	12	(100000)
					$[(32\bar{1}002)?]$
20	32	$(20120\bar{1})$	(0/0 2/4 0/0)	30	(110000)
22	33	$(21120\bar{1})$	(0/1 2/4 1/0)	120	
24	36	(222000)	(2/2 2/2 2/2)	20	(220002)
		$(21121\bar{1})$	(0/2 2/4 0/0)	60	$[(5610\bar{3}3)?]$

tor, and the two are related by Eq. (9). For powder pattern intensities the multiplicity of each spot is given. The sequences of our indexing of course satisfies Eq. (13) relating N to the sum of squares of indices. As was noted earlier, the list[11] of powder diffraction angles correlates perfectly with this sequence, with only one omission in this range.

The last column gives the indexing of Ref. 11. The fundamental (100000) vector was chosen in Ref. 11 to have the length of $Q_0(18)$. As a result, all smaller reflections become higher index and the simple monotonic relation between N and Q of Eq. (13) is lost. Because of this there is no obvious start to the sequence, and it is difficult to know if any intense spots are missing. Furthermore, because of the incommensurability one can approach any angle with arbitrary precision by using high indices. The two assignments[11] labelled with question marks are probably such approximations. The question of which vector one chooses as a fundamental length in this case is uniquely resolved by the sequence of the intense reflections. Choosing a longer vector leads to the problems cited above. It will be difficult to choose a shorter vector, because intensities are likely to be very low.

We have so far concentrated on the Q_0 series. Table V lists representative spots for all the spots that occur for $N = 12$ spherical shell in six dimensions (Fig. 9). Two types of indices sum to $N = 12$. In six dimensions there are 2^6 spots of type (111111) and $2^3 6!/(2!3!)$ of type (211000). Six different lengths result from projecting in three dimensions ranging from $Q_0^2 = 37.89$ to $Q_5^2 = 5.53$. The longer Q's are from six-dimensional vectors nearly parallel to the cut plane; the shorter ones are from those nearly perpendicular. By themselves the (n_i) give no clue about projected length until the projection has been defined in Eq. (20), but in the cubic indexes the lengths obviously become shorter as the 2's shift from primed to unprimed positions and sign differences appear in the indexes.

The (111111) are high symmetry axes in six dimensions. They project into three dimensions as either three- or fivefold axes with four different lengths. The (211000) project onto mirror planes or (110) planes with six different lengths. In powders the Q_0 (12) reflection will be a superposition of 72 individual diffraction spots. These multiplicities are most readily apparent by forming ratios of the cubic indices and comparing these with the indexes of the three symmetry axes and the mirror planes.

We hope to have demonstrated that the cubic coordinate system has many advantages over either the skew coordinate system or the six-dimensional one. In addition, there is an obvious simplification when a particular lattice constant is chosen.

VIII. DISCUSSION

Several indexing methods have been introduced and need to be compared. We have introduced a method of indexing based on a three-dimensional cubic coordinate system using icosahedral symmetry. Six indexes are necessary and sufficient, indicating that the icosahedral solid is quasiperiodic and can be represented as an irrational cut of a six-dimensional periodic solid. Much of the geometry is developed without recourse to six dimensions.

The six-index notation is merely a shorthand for indexing irrational numbers of the form $h + h'\tau$. Ordinary vector addition generates the three-dimensional diffraction pattern from a single vector replicated by the

operations of the icosahedral group. There is a single basic length: the $\pi/5$ rotations introduce the algebraic number τ and, therefore, incommensurability. Unlike other incommensurate structures, in which the incommensurate ratio varies with temperature and composition, the ratio τ is part of fivefold rotation and remains the same for large changes in composition[15] and lattice parameter and a wide variety of alloy systems. The cubic coordinate system has many advantages that derive from an orthogonal coordinate system. It incorporates the cubic subgroup part of the icosahedral symmetry, but it leaves the problem of multiple notation for equivalent positions.

The multiple notation is really not a problem. We have found two convenient methods. For a particular index, multiplication by the rotation matrices quickly gives all the other notations for equivalent reflections. When dealing with a large number of indexed positions, they are quickly sorted by calculating Q^2 and sorting by N and M (or r). Just as (330) and (411) coincide in bcc powder patterns, this sorting will put nonequivalent spots in the same (N,r) box. However, since all the spots in the same (N,r) box originate from the spots in the six-dimensional reciprocal space that are the same distance from the cut plane, they are likely to have similar intensities. The other three-dimensional coordinate systems have skewed axes aligned along equivalent symmetry axes. They have all the problems of skewed axes including the problem that permutation of indices not only cause length changes but can cause the vector to rotate to a nonequivalent direction. In the cubic indexing, because the indices are primed and unprimed, cyclic permutations of (HKL) can only lead to equivalent vectors. Odd permutations do not change the length.

In six dimensions there is an orthogonal system, but the rotation matrix that defines the cut plane requires arbitrary choices of the signs of the fivefold basis vectors in three dimensions. Thus the various six-dimensional vectors of type (110000) represented two different lengths in three-dimensions differing by a factor of τ, depending on the relative orientation with respect to the cut plane, or equivalently whether the angles between the various (100000) type (010000) vectors in three dimension are acute or obtuse.

There is a geometric way of understanding the discrepancy between the various indexing methods. It might seem that any reflection along the fivefold axis could serve to define the unit length, but it must satisfy several criteria. The first is that all other spots must then be indexable with six integers that obey the parity rules. The spots that survive this criterion differ from each other in length by powers of τ^3. In six dimensions all of these vectors lie on the same $(xyyyy\bar{y})$ fivefold plane. The shortest distance in this plane is (100000) and this is the one which must be found. Only one of the fivefold reflections corresponds to this minimum distance and generates an orthogonal basis in six dimensions. The one chosen in Ref. 11 happens to be the $(21111\bar{1})$, which leads to a skewed six-dimensional basis. This destroys the hypercubic geometry that is so important to the simplicity of the indexing we have proposed. As a result the indexing fails to fit the criterion of a simple hierarchy. There are inifinitely many reflections along the fivefold axis, both longer and shorter than the one which meets this criterion. For the P quasilattice, it is the longest fivefold reflection that is shorter than any intense reflection in any direction. All shorter reflections are then projections of longer six-dimensional vectors with long Q_c and weak intensities.

These criteria not only point to a natural and unique indexing but solves the important problem of what constitutes the unit reciprocal lattice vector. Comparison of Table V indicates that while a different choice of this unit still gives a completely consistent set of indexing, there is a simplicity and completeness to the choice based on the strong reflections. The Q_0 series fits the observed intense reflections without omission and, qualitatively, is inversely correlated with Q_c, the distance from the cut plane. The next in the sequence (Table VI) $Q^2(N,1) = Q_0^2(N) - 4\tau$ all have $Q_c > 2\sqrt{\tau}$ which, of course, is longer than Q_c for any of the Q_0 spots, and are readily distinguished from the main sequence by their

TABLE VI. A complete listing of the $N = 12$ reflections.

	M	(n_i)	$h/h'\,k/k'\,l/l'$	Multiplicity
$Q_0(12)$	16	(210010)	(2/2 0/2 0/0)	60
		$(11111\bar{1})$	(0/2 2/2 0/0)	12
$Q(12,1)$	12	$(1111\bar{1}1)$	(0/2 0/2 0/2)	20
		$(20100\bar{1})$	(2/0 2/2 0/0)	60
$Q(12,2)$	8	(201001)	(2/0 0/2 0/2)	120
$Q(12,3)$	4	$(2100\bar{1}0)$	(2/0 0/2 2/0)	120
$Q(12,4)$	0	$(111\bar{1}\bar{1}\bar{1})$	(2/0 2/0 2/0)	20
		(010210)	$(\bar{2}/2\ 0/2\ 0/0)$	60
$Q(12,5)$	-4	$(\bar{1}11111)$	$(\bar{2}/2\ 2/0\ 0/0)$	12
		$(20\bar{1}001)$	$(2/0\ \bar{2}/2\ 0/0)$	60

weak intensity. Our indexing method therefore uniquely identifies the quasilattice parameter d_0 in a way that is quite equivalent to that chosen by Elser[12] based on an examination of the Fourier transform of the cut function along a systematic row. Because our method is purely geometric and does not refer to any specific cut function, it is in a sense more general.

In this paper we have taken for granted that the symmetry is truly icosahedral. The choice of the cubic axes for a coordinate system does not imply that we believe that this is a cubic crystal, as has been suggested by others.[16,17] We will address this issue in a separate paper.[18]

ACKNOWLEDGMENT

We wish to thank DARPA for sponsoring this study.

REFERENCES

[1]D. Shechtman, I. Blech, D. Gratias, and J. W. Cahn, Phys. Rev. Lett. **53**, 1951 (1984).
[2]D. Shechtman and I. Blech, Met. Trans. **16A**, 1005 (1985).
[3]L. Bendersky, Phys. Rev. Lett. **55**, 1461 (1985).
[4]T. Ishimasa, H. U. Nissen, and Y. Fukano, Phys. Rev. Lett. **55**, 511 (1985).
[5]H. A. Bohr, *Almost Periodic Functions* (Chelsea, New York, 1947).
[6]A. S. Besicovitch, *Almost Periodic Functions* (Cambridge U.P., London, 1932).
[7]P. Kramer and R. Neri, Acta Cryst. A **40**, 580 (1984).
[8]M. Duneau and A. Katz, Phys. Rev. Lett. **54**, 2688 (1985).
[9]V. Elser, Phys. Rev. Lett. **54**, 1730 (1985); Acta Cryst. A (to be published).
[10]P. A. Kalugin, A. Yu Kitayev, and L. S. Levitov, J. Phys. Lett. **46**, L601 (1985).
[11]P. A. Bancel, P. A. Heiney, P. W. Stephens, A. I. Goldman, and P. M. Horn, Phys. Rev. Lett. **54**, 2422 (1985).
[12]V. Elser, "Introduction to Quasicrystals," Acta Cryst. A (to be published).
[13]D. B. Nelson and S. Sachdev, Phys. Rev. B **32**, 689, 1480 (1985).
[14]D. Levine and P. Steinhardt, Phys. Rev. Lett. **53**, 2477 (1984).
[15]R. J. Schaefer, L. A. Bendersky, D. Shechtman, W. J. Boettinger, and F. S. Biancaniello, submitted to Met. Trans.
[16]M. Kuriyama, G. G. Long, and L. Bendersky, Phys. Rev. Lett. **55**, 849 (1985).
[17]L. Pauling, Nature **317**, 512 (1985).
[18]J. W. Cahn, D. Gratias, and D. Shechtman, Nature **319**, 102 (1986).

JOURNAL DE PHYSIQUE
Colloque C3, supplément au n°7, Tome 47, juillet 1986

QUASIPERIODIC CRYSTALS - EXPERIMENTAL EVIDENCE

D. SHECHTMAN*(1)

Materials Science and Engineering, The Johns Hopkins University, Baltimore, MD 21218, U.S.A.

Abstract- A review of the experimental evidence which rejects the determination of the Icosahedral phase as periodic is presented. The experiments discussed include various diffraction techniques for the study of the long range order as well the methods to determine the local atomic arrangement.

I - INTRODUCTION

The discovery of the Icosahedral phase (1), (2) has generated a great deal of research activity. It is the fascination of being a part of an emerging new field, which motivated investigators from several disciplines to contribute about 150 articles in the first year. However, a certain amount of mainly passive scepticism still exists within the ranks of crystallographers.

Since the first X-ray diffraction Experiment by von Laue in 1912, all crystals studied by various techniques could be defined as periodic. Many structures were analysed to have rather complicated motifs and large unit cells, which contain in several cases well over a thousand atoms, (Frank-Kasper phases are a typical example).

All these, however, could be shown to have periodic translational symmetry. Therefore, a crystal which generates sharp diffraction peaks was axiomed over the years to be periodic. This axiom which has become a cornerstone in crystallography is not supported by the mathematics of the nature of diffraction. On the contrary, it was demonstrated and proved time and again that the Fourier transform of almost periodic and quasiperiodic functions also generate sharp peaks.

The question whether quasiperiodic crystals exist, narrows down to the question whether quasiperiodic arrangement of atoms can form and whether it can be stable.

The mathematical as well as other theoretical and experimental tools, to deal with quasiperiodic crystals, were available for quite some time before the announcement of the discovery of the Icosahedral phase, and these were put to use almost immediately following the announcement.

---

*Permanent address : Department of Materials Engineering, Israel Institute of Technology, Technion, Haifa, Israel

(1)Guest Worker, National Bureau of Standards, Gaithersburg, MD 20899, U.S.A.

The experiments that revealed the exceptional nature of the Icosahedral phase were repeated and this not only confirmed the first results, but also expanded them and added evidence for quasiperiodicity in the Icosahedral phase and other phases (3)(4). The phase, first found in several aluminum alloys (5) was later discovered in other compositions (6).

The purpose of this article is to discuss experimental evidence which rejects the possibility of explaining the structure of the Icosahedral phase on principles of classical crystallography, thus creating the foundation for the understanding of the structure of quasiperiodic crystals.

EXPERIMENTAL

There is no doubt that electron microscopy, with its versatility and wealth of experimental procedures, played a key role in the early stages of the study of the Icosahedral phase and other quasiperiodic structures.

The property that drew attention to the fivefold orientation in April 1982 was the very dark image of the Icosahedral grains which were oriented with the fivefold axis parallel to the electron beam. The Icosahedral phase diffracts electrons in an unusual way.

Next came the diffraction pattern (Fig.1), with well defined sharp peaks and fivefold rotational symmetry. The pattern has more unique features, the distances from the centrally transmitted beam to the diffracted beams are related by various powers of the golden mean and the intensity of the diffracted beams does not decay as a function of the distance from the center. But, perhaps, the most intricate observation was that the crystal, in different orientations, has more such fivefold diffraction patterns. The analysis of the symmetries of the crystal lead to the composition of patterns shown in Fig.2 and to the realization that the crystals possess Icosahedral symmetry. The explanation of the previously unobserved set of symmetries could be either by using the knowledge of traditional periodic crystallography or by proposing something else and new.

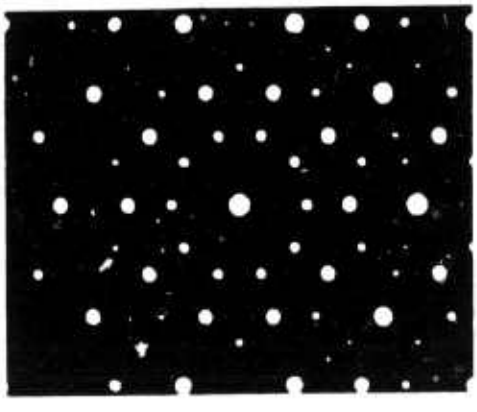

Fig.1. Selected area diffraction Pattern taken from a single Icosahedral Crystal (1).

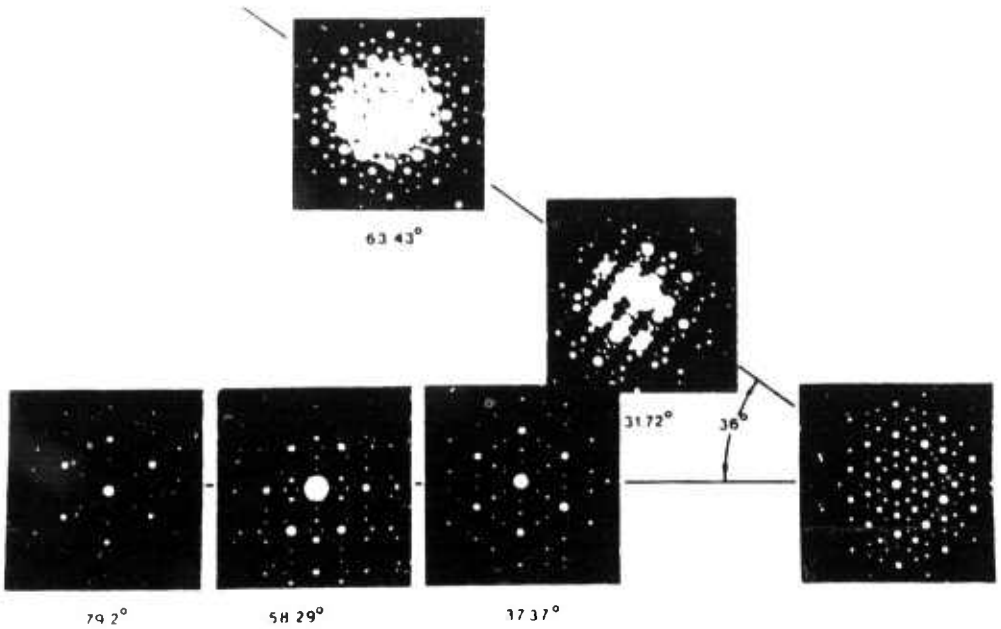

Fig.2. The sequence of selected area diffraction patterns obtained from one Icosahedral crystal at various tilt angles (1).

Periodic crystallography may suggest that each spot in the unique patterns is formed by a contribution of several differently oriented particles of a periodic phase, such as multiple twinning. To examine this idea several experiments were carried out in the electron microscope. The first is a set of dark field images obtained from different diffracted beams in a two-beam condition (1). In each dark field image the whole Icosahedral grain was illuminated, and down to the resolution of a few nanometers, no twins can be observed. This experiment was repeated since on various other Icosahedral phases, some of which (such as several rapidly solidified Al-Mn-Si alloys) are with much less strain contrast with the same results (7).

Convergent beam diffraction patterns were taken at the various important orientations. This technique involves a conical electron beam that illuminates a spot on the specimen, the diameter of which is between 1.5nm to 20 nm. The diffraction patterns obtained this way are identical to the ones observed by the selected area method, and are similar to one another across the Icosahedral crystal. Such selected area diffraction patterns were taken at various thicknesses of the specimen, and down to a few nanometers in thickness, indicating that if, indeed, the diffraction pattern is a composite of several patterns obtained from several periodic crystals, then these crystals must be very small.

Perhaps, the most convincing set of experiments in the stuuy of the structure of the Icosahedral phase is based upon lattice imaging. The lattice imaging technique has been used extensively in the last decade to study lattice defects. It has been demonstrated that the technique can detect the fine structure of dislocation cores and that of many kinds of boundaries, including microtwin boundaries (8). The

technique was applied to the Icosahedral phase in several alloys (9) revealing the atomic structure at different orientations. Even though it is difficult to confirm a structural model based on these observations, several facts are clear. The most important observation is that no boundaries can be seen in the structure. The quasiperiodic sequence of planes is clearly seen, and the orientations of planes in the 2-, 3- and 5-fold orientation is conspicuous. An optical diffraction taken from the TEM plate to form a Fourier transform of the image recreates the electron diffraction pattern. This result is obtained even with a rather small aperture, i.e. with the diameter of the area which contributes to the optical diffraction in the order of several nanometers. The various rotational symmetries, including the fivefold, are thus a fundamental property of the atomic order and do not result from any composition of small periodic crystals, such as microtwins.

X-ray diffraction has traditionally been a most powerful and precise tool in the study of crystals. The technique was put to use in the study of the quasiperiodic crystals, starting with the Icosahedral phase (1)(5)(10). The fit of the X-ray diffraction peaks to those of the electron diffraction was confirmed, and the indexing of the patterns followed soon (5)(11). Even though there is no dispute as to the meaning of each peak among the various suggestions for indexing languages, the indexing techniques vary from one to the other. The most fundamental of all is the one suggested by Cahn et al (11). It is based upon a set of three orthogonal 2-fold axes and presents an easy and workable indexing system. Another important result of the analysis of the X-ray diffraction patterns is the introduction of the step necessary to prove, using diffraction, that a solid is quasi-periodic.

Among the other results obtained by X-ray diffraction is the accurate measurement of planar spacing, which is not obtainable accurately by electron diffraction, and the introduction of indexed stereographic projections for the Icosahedral phase (11). In general, the peaks observed in all the X-ray studies are rather wide representing a correlation length of 10-30nm. Numerous speculations as to the cause of this width have been presented including local strain, faults and uneven distribution of atomic constituents to name a few. This question is unsettled at present and an agreed upon explanation is still sought.

Neutron diffraction on powdered Icosahedral phase was also performed on three alloy compositions (12). Peak positions were found at identical positions to those previously found by X-ray diffraction and previously as produced by cuts and projections of a 6D cube with a lattice parameter of about 0.65nm (see later in these proceedings). The intensities of the neutron diffraction pattern provide information on the chemical order of the Icosahedral phase by comparison to those of the X-ray diffraction pattern. This is based upon the difference between the structure factors characteristic of the two techniques, which is vividly demonstrated for the Al-Mn system.

The local atomic structure of the Icosahedral phase was studied by NGR, XAFS and NMR.

Shortly following the discovery of the Icosahedral phase Nuclear Gamma-Ray Resonance (NGR) experiments were performed on Al- (Mn,Fe) alloys (13). The NGR spectrum of an iron atom in the Icosahedral phase is a probe of the local environment of that atom and the technique is most sensitive to the first one or two near-neighbor shells. A detailed analysis of the spectra obtained from the

Icosahedral structure shows that they can be fitted to a pair of symmetric doublets, indicating two non-symmetric positions for the iron atom. It is assumed that the iron and manganese atoms occupy the small site types and are distributed arbitrarily within the quasi-periodic crystal. The results do not suggest a model, but reject any model in which the manganese atom occupies a symmetric position.

In another study (14) the local atomic environment in the Icosahedral phase was studied by Extended X-ray Absorption Fine Structure (EXAFS) measurements. The results which provide information that lead to a structural model, demonstrate the power of this tool for the study of the order of the Icosahedral phase. The model, detailed in these proceedings, supports the randomly connected Icosahedra model previously suggested (1) and suggests a structural unit which consists of a cage of Mn atoms positioned on the vertices of an Icosahedran. The model also suggests that the quasiperiodic crystals grow along the threefold axis, which is consistent with previously reported optical microscopy observations (10).

Nuclear Magnetic Resonance (NMR) is a technique which probes the local environment of the nuclei. In their study (15) both 55Mn and 27Al nuclei were examined at room temperature. One of the conclusions of this study supports the conclusion of the Mossbauer spectroscopy (NGR) study (13a).

A direct observation of the atomic structure of the Icosahedral phase was performed by Field Ion Microscopy (FIM) (16). The results confirm the long-range Icosahedral orientational order without trans- lational symmetry. The basic rotational symmetries were observed in real space, and the results confirm the long-range Icosahedral orientational order without translational symmetry.

In addition, a large number of apparent discontinuities were found. Special attention was paid to the possibility of the presence of twins, but no evidence was found for multiple twinning, and no twin boundaries were observed. It should be noted that the FIM studies were performed on a rapidly solidified ribbon of Al-12 at % Mn, which is by nature heavily strained. A more suitable specimen for this study would be a rapidly solidified ribbon of the Al-Mn-Si ternary system which is composed of elongated strain free Icosahedral crystals.

Based on the FIM, several laboratories have now developed an atom probe which is potentially an important tool for probing the chemical order of the Icosahedral phase, and for evaluating the models for its atomic structure.

CONCLUSION

Many of the techniques for the study of the structure of solids were applied to the Icosahedral phase. The long range order was determined by X-ray, neutron and electron diffraction, and a very good fit was obtained for a three dimensional quasiperiodic arrangement of atoms. The local order was probed by field ion microscopy, nuclear gamma-ray resonance, nuclear magnetic resonance and extended X-ray absorption fine structure. At this stage the available information on the local order should provide a model for the atomic arrangement both of the Icosahedral phase in particular, and for quasi- periodic crystals in general. Indeed, such models are proposed in these proceedings, and hopefully an agreed upon model will emerge in the near future.

ACKNOWLEDGEMENT

The author wishes to thank DARPA and ONR for their support of this work.

REFERENCES

/1/ Shechtman, D. and Blech, I.A., Metallurgical Transactions , 16A P. (1985) 1005-1012.
/2/ Shechtman, D., Blech, I.A., Gratias, D. and Cahn, J.W., Physical Review Letters V.53 No. 20 P (1984) 1951-1953.
/3/ Bendersky, L.A., Phys. Rev. Letters, V.55 (1985) 1461.
/4/ Ishimasa, T., Nissen, H.U. and Fukano, Y., Physical Review Letters Vol.55 No.5 (1985) 511-513.
/5/ Bancel, Peter A., Heiney, Paul A., Stephens, Peter W., Goldman, Alan I. and Horn, Paul M., Physical Review Letters V.54 No.22 (1985) 2422-2425.
/6/ Poon, S.G., Drehman, A.J. and Lawless, K.R., Phys. Rev. Lett 55 (1985) 2324.
/7/ (a) Bendersky, L.A. and Kaufman, M.J., Preprint.
(b) Chen, C.H. and Chen, H.S., Preprint.
/8/ Kuo, K.H., Preprint.
/9a/ Shechtman, D., Gratias, D. and Cahn, J.W., Comptens Rendus Series II V.300 (1985) 909.
/9b/ Portier, R., Shechtman, D., Gratias, D., Bigot, J. and Cahn, J.W., Institute Phys. Conf. Series No.78 Adam Hilger Chap.9 (1985) 317-320E.
/9c/ Hiraga, K., Hirabayashi, M., Inoue, A. and Massumoto, Tsuyoshi, Sci. Rep. Ritu AV. 32 No.2 (1985) 309-314.
/9d/ Hiraga, Kenji, Hirabayashi, Makoto, Inoue, Akihisa and Masumoto, T., J. of the Physical Soc. of Japan Vol.54 No.11 (1985) 4077-4080.
/9e/ Hiraga, K. and Hirabayashi, M., Proc. Int. Sym. on Science of Form (1st:1985: Tsukuba).
/9f/ Ball, M.D. and Lloyd, D.J., Scripta Metallurgica V.19 (1985) 1065-1068.
/9g/ Knowles, K.M., Greer, A.L., Saxton, W.O. and Stobbs, W.M., Philosophical Magazine B. Vol.52 No.1 (1985) L31-L38.
/9h/ Gronsky, R., Krishnan, K.M., Tanner, L.E. and Bailey, G.W., "Proceedings EMSA annual meeting" (43: 1985: Louisville Kentucky) San Francisco Press (1985) 3.
/10/ Schaefer, R.J., Bendersky, L.A., Shechtman, D., Boettinger, W.J. and Biancaniello, F.S., submitted to Met. Trans A.
/11/ Cahn, J.W., Shechtman, D. and Gratias, D., J. of Materials Science Vol.2 (1986).
/12/ Mozer, B., Cahn, J.W., Gratias, D. and Shechtman, D. These proceedings.
/13a/ Swartzendruber, L.J., Shechtman, D., Bendersky, L.A. and Cahn, J.W., Physical Review B.Vol.32 No.2 (1985) 1383-1385.
/13b/ Eibschutz, M., Chen, H.S. and Hauser, J.J., Physical Review Letters V.56 No.2 (1986) 169-172.
/14/ Stern, E.A., Ma, Y. and Bouldin, C.E., Phys. Review Letters V.55 No.20 (1985) 2172-2175.
/15/ Rubinstein, M., Stauss, G.H., Phillips, T.E., Moorjani, K. and Bennett, L., J. of Materials Research Vol.1 No.2 (1986).
/16/ Melmed, A.J. and Klein, R., Preprint.

COMMENTS AFTER THE D. SHECHTMAN TALK :

M.V. JARIC.- I would like to make two comments. First, I would like to emphasize that SHECHTMAN's model of randomly packed icosahedra sharing edges, faces, or vertices, does, in fact, exhibit an unusual kind of order - namely, the long-range icosahedral orientational order. Second, I think that a selfconsistent definition of a class of (long-range positionally) ordered structures could be a physical one : these are (infinite) structures which give rise to diffraction patterns consisting of perfectly sharp bragg peaks. It would be, then, an experimental task to recognize this ideal in real structures.

Neutron Diffraction Studies of the Icosahedral Phase of Al-Mn Alloys

B. Mozer (+), J. W. Cahn (+), D. Gratias (++), and D. Shechtman (+++)

(+) Center for Material Sciences, NBS, Gaithersburg, MD 20899, U.S.A.

(++) C.E.C.M/C.N.R.S. 15 rue G. Urbain 94400-Vitry, France

(+++) Dept. of Material Engineering, Israel Institute of Technology, Technion, 32000 Haifa, Israel and the Dept. of Materials Science and Engineering Johns Hopkins University, Baltimore, Maryland, U.S.A.

Abstract - Powder neutron diffraction studies were performed on three icosahedral alloys of the aluminum manganese system containing 27, 30, and 34 weight percent manganese. All peaks were found at the angles consistent with the icosahedral indexing with a six-dimensional cubic lattice parameter of approximately 0.65 nm that decreased with increasing Mn content. The relative intensities differ significantly from those found for X-rays. The intensities are not consistent with a quasilattice consisting of the 3-dimensional Penrose tiling with a .46 nm edge length along the 5-fold axis. It is consistent with a 1.0 nm edge along the 3-fold axis quasilattice node separation.

I - INTRODUCTION

Since the discovery of the icosahedral phase in rapidly solidified melt spun ribbons of Al-Mn alloys /1,2/, a number of experimental techniques have been used to determine the structure of these aperiodic systems. In the original work, electron diffraction studies were made on small regions of the ribbon where the icosahedral phase was singly oriented. Further studies showed the presence of other phases coexisting with the icosahedral phase./3,4/ Depending on the concentration of manganese, the cooling rate, heat treatment, etc., one can find the icosahedral phase, the α-aluminum phase, or the decagonal phase /5/ in many combinations. We report here on some powder neutron diffraction studies of the aluminum manganese icosahedral phase since no large singly oriented single phase specimens are available. We studied this phase using powdered specimens of several compositions of the alloys. Other powder diffraction patterns were obtained for powders containing the icosahedral phase and the decagonal phase and for powders annealed to produce the equilibrium orthorhombic Al_6Mn.

II - SAMPLE PREPARATION

Melt spun ribbons were obtained [1] from each of these $Al_{1-x}Mn_x$ alloys where x corresponded to 27 [2], 30, and 34 [3] weight percent of the pure starting

(1) We thank Dr. A. Rabinkin of the Allied-Signal Corporation for providing us these samples.

(2) This corresponds to Al_4Mn

(3) This corresponds to Al_6Mn

Les Editions de Physique (1986) (Accepted for publication)

materials . The ribbons were then gently powdered so as not to introduce excessive strain and sieved to provide the neutron diffraction samples.

III - EXPERIMENTAL PROCEDURE

Neutron diffraction measurements were performed on the high resolution BT-1 powder diffractometer /6/ at the NBS 20-MWatt research reactor. The diffractometer consists of 5 separate counters, separated by 20°, that can move simultaneously about an axis at the sample position. The 5 counters cover an angular range from 0° to 120° and for our experiments covered from 5° to 120° scattering angle where each counter moved 35°. The wave length used for our experiments was 1.546Å provided by a copper monochromator. An oriented graphite filter was used in the beam to remove higher order wave lengths contamination. The resolution of the diffractometer varies over the scattering angle from 0.31° at 5° scattering angle to a minimum of 0.22° from 40° to 70° and rises to 0.58° at the largest scattering angle.

The powder to be studied is placed in a thin walled vanadium container which can be fixed at the sample position. Vanadium was used since it does not contribute any structure to the diffraction patterns. Diffraction data was taken for each powder in angular steps of 0.05° and for a given monitor count of the incoming beam.

IV - RESULTS

Figure 1 shows a comparison of the diffraction data versus scattering angle for the three alloys with manganese concentration increasing from the top to the bottom graph. The lowest concentration manganese alloy when melt spun under the conditions for our experiment produces the icosahedral phase plus the f.c.c. α-aluminum. The α-aluminum phase lines in our pattern are narrower than the peaks of the icosahedral peaks but do not completely reflect the instrumental resolution. Their width could arise from particle size broadening or possible broadening caused by non-uniform concentration of Mn in the α-aluminum phase. The icosahedral lines although quite sharp compared to other samples we have examined are broadened significantly more than our resolution function. One also notes an oscillatory background under the peaks of the icosahedral phase. This oscillatory background is reminiscent of the behavior of binary alloy systems showing short range order or possibly the presence of an amorphous phase in our system. No amorphous phase was detected by TEM. An examination of the background behavior at the smaller angles seems to indicate a pattern similar to short range order since the curve is tending upward away from zero. An experiment is being designed to probe these smaller angles to attempt to further clarify this point.

One sees in the neutron diffraction a slight shift in peak positions versus the manganese concentration. This has been observed by both electron and x-ray diffraction./4/ With increasing manganese content there is a change in the amount of other phases present; α aluminum is reduced and the decagonal phase appears. (Neither the Al_6Mn nor Al_4Mn phases were observed.) These changes are observed in the region from 22° to 45° in two theta but can be seen to occur over most of the pattern. We are attempting to prepare a sample in the pure decagonal phase and to measure its neutron, electron and x-ray diffraction patterns in order to analyze completely the diffraction curves with mixed aperiodic phases.

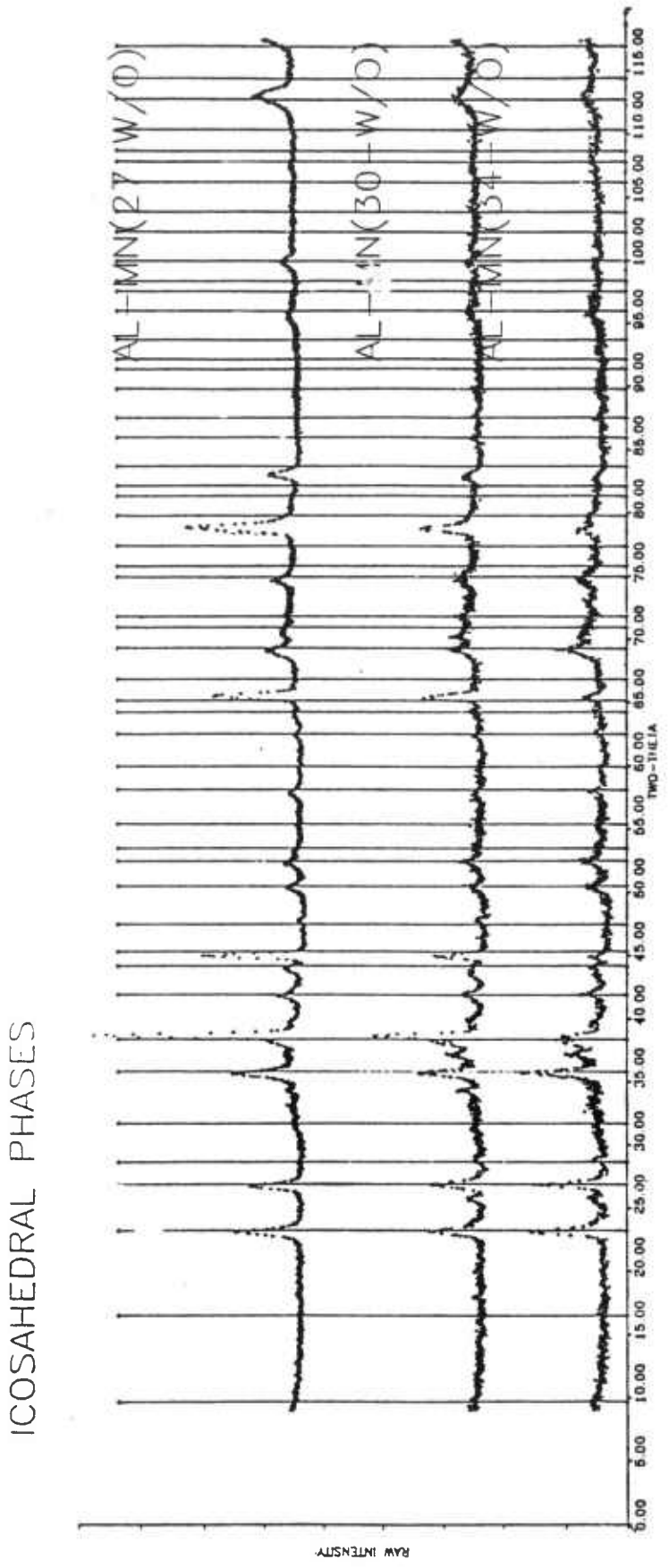

Fig. 1 - The uncorrected neutron scattering intensity of the 3 alloys, Mn(27w/o), AlMn (30 w/o), and AlMn (34 w/o), from top to bottom respectively versus the scattering angle, 2θ. The vertical lines are the predicted positions of the Q_o series of icosahedral lines for all even values of N between 2 and 106.

Figure 2 shows a comparison of a powder neutron diffraction pattern of the icosahedral phase with the X-ray diffraction pattern /7/ for a similar alloy. The most interesting feature is the difference in the intensities for the same icosahedral peaks. Furthermore, many peaks are observed in the neutron diffraction pattern that seem to be absent in the X-ray pattern, whereas, some strong X-ray peaks are very weak in the neutron pattern. This striking difference in intensity comes from chemical order and the difference in phase of the neutron scattering amplitudes of the manganese atoms which have a negative neutron scattering length relative to that of aluminum.

In the preliminary analysis of the neutron diffraction data for the 27% alloy, we obtained the integrated intensity under all icosahedral peaks positions calculated from the index method we discuss later. To obtain the integrated intensity we did not attempt at this point to fit peak profiles with assumed mathematical forms but subtracted a smooth background from each peak and numerically integrated the resultant intensity. For some positions the intensity differed little from background. These were listed as zero intensity and utilized because they too contain information. In the case of the few overlapping peaks, where the separation could be clearly made, we adjusted each peak's intensity to give it a smooth symmetrical curve whose summed intensity agreed with that observed. Peaks that overlapped with those of other phases were not measured. In order to compare the experimental intensities with our model, we corrected the above integrated intensities by multiplying it by $\sin^2\theta \cos\theta$, the applicable Lorentz factor for neutron scattering, where θ is one-half the scattering angle. Finally for a comparison with our model we divided each integrated intensity with its multiplicity as determined by the model and normalized these intensities so that the largest one would be unity. For those cases where several nonequivalent peaks had identical θ, the intensity was divided by the sum of the multiplicities.

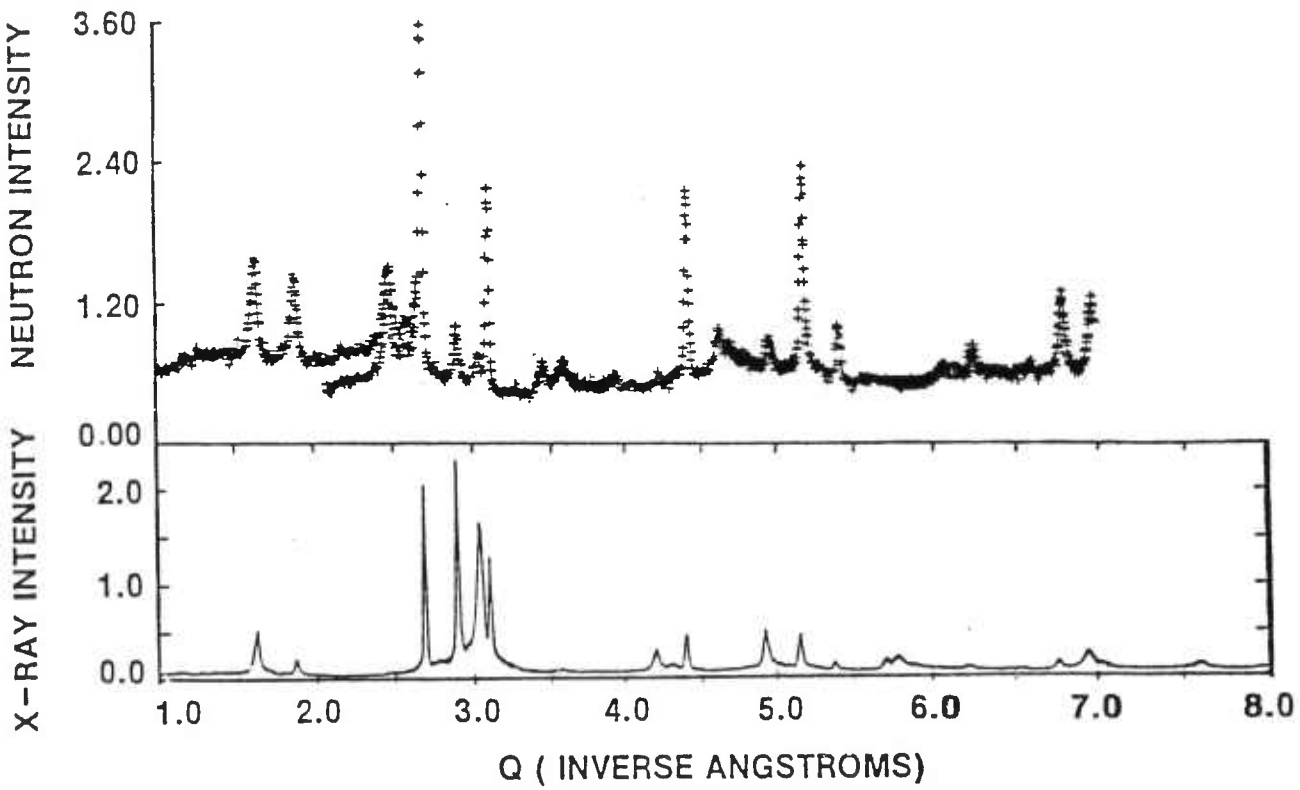

Fig. 2 - A comparison of the uncorrected neutron scattering intensities, top, to the scattering intensities for x-rays /7/ versus $Q = 4\pi\sin\theta/\lambda$ where θ is one-half the scattering angle and λ is the wave length of the radiation used. The two curves in the neutron data near Q=2.3 reflect the overlapping range of the detectors

V - DISCUSSION

Two aspects of the neutron diffraction results will be discussed; peak positions and how this relates to the icosahedral symmetry, and intensity and how this confirms the emerging model of a structure of parallel large icosahedral motifs stacked aperiodically along their 3-fold axes.

VI - COORDINATE SYSTEMS

The geometries of both the direct and reciprocal spaces in three dimensions are conveniently described in terms of a Cartesian coordinate system aligned with one set of three mutually orthogonal 2-fold axes which occur in icosahedral symmetry./8/ Each of the three components of a quasilattice or reciprocal quasilattice vector will be described in terms of two integers e.g., h and h', the magnitude of the component is $h + h'\tau$ where

$$\tau = 2\mathrm{Cos}(\pi/5) = (1 + \sqrt{5})/2 = 1.618034.$$

A reflection Q is indexed with six integers ($h + h'\tau$, $k + k'\tau$, $l + l'\tau$) which will be written (h/h' k/k' l/l'). Similarly a translation vector X will be written (u/u' u/u' w/w'). These six integers can also be related to components $(x_1 x_2 \ldots x_6)$ of a six-dimensional lattice vector in Z^6 or components $(n_1 n_2 \ldots n_6)$ of a reciprocal lattice vector in Z^{*6} by the equations:

$$\begin{aligned} h &= n_1 - n_4 & h' &= n_2 + n_5 \\ k &= n_3 - n_6 & k' &= n_1 + n_4 \\ l &= n_2 - n_5 & l' &= n_3 + n_6 \end{aligned} \qquad (1)$$

with similar equations relating u,u'...w' to the x_i.

Equation (1) can be considered to define a projection of Z^6 onto a three dimensional plane. It will be convenient to let the (100000) vectors in Z^6 and Z^{*6} have a unit length. Then the corresponding vectors in R^3 along the 5-fold axis (1/0 0/1 0/0) will have a projected length $1/\sqrt{2}$. We therefore normalize all three-dimensional vectors by a factor of $\sqrt{2(2 + \tau)}$. In our previous paper /8/ the vector (1/0 0/0 0/0) in R^3 was chosen to have unit length. As a result of the redefinition of a unit length formulas for lengths in this paper differ from that of the previous paper by a factor of $2(2+\tau)$.

$$Q = 1/\sqrt{2(2 + \tau)}\ ((h + h'\tau)i + (k + k'\tau)j + (l + l'\tau)k)$$

$$X = 1/\sqrt{2(2 + \tau)}\ ((u + u'\tau)i + (k + k'\tau)j + (l + l'\tau)k)$$

Note that X (1/0 0/1 0/0)·Z(1/0 0/1 0/0) = 1/2. These vectors which were reciprocal to each other in Z^6 have been foreshortened by projection and are no longer reciprocal to each other. To convert these to dimensional quantities **x** and **q** we will use the six-dimensional cubic lattice parameter A an reciprocal lattice parameter $A^* = 1/A$ and let

$$\begin{aligned} \mathbf{x} &= A\mathbf{X} \\ \mathbf{q} &= A^*\mathbf{Q} \end{aligned} \qquad (2)$$

For powder diffraction we need only the magnitudes of these vectors. Because $\tau^2 = 1 + \tau$ these become

$$Q^2 = (N + M\tau)/2(2 + \tau) \qquad X^2 = (S + T\tau)/2(2 + \tau) \tag{3}$$

and where

$$N = 2\Sigma n_i^2 \qquad\qquad S = 2\Sigma x_i^2$$

$$= h + h'^2 + k^2 + k'^2 + l^2 + l'^2 \qquad = u^2 + u'^2 + v^2 + v'^2 + w^2 + w'^2 \tag{4}$$

$$M = h'^2 + k'^2 + l'^2 + 2(hh' + kk' + ll') \qquad T = u'^2 + v'^2 + w'^2 + 2(uu' + vv' + ww') \tag{5}$$

Hence N and S are always even. Furthermore if N(or S) is divisible by 4, so is M(or T). If N(or S) is of the form 4m + 2, M(or T) is of the form 4m + 1. In addition we have

$$-N/\tau < M < N\tau \qquad -S/\tau < T < S\tau. \tag{6}$$

Equation 4 states that all vectors with the same value of N (or S) lie on the same sphere in Z^{*6} (or Z^6). The distance Q_c that a reflection in Z^{*6} is from the icosahedral cut plane defined by equations (1) is given by

$$Q_c^2 = \tau(N\tau - M)/2(2 + \tau) \tag{7}$$

Thus the largest possible value of M for a given N will have the smallest Q_c and usually the greatest intensity. This largest value of M is called M_o. The corresponding value of Q is called Q_o and is a one parameter sequence of reflections.

$$2(2 + \tau)\, Q_o^2 = \begin{cases} N + 4\tau\left\lfloor N\tau/4 \right\rfloor & N=4n \\ N + \tau\left(1 + 4\left\lfloor \frac{N\tau - 1}{4} \right\rfloor\right) & N=4n+2 \end{cases} \tag{8}$$

where $\lfloor X \rfloor$ is the largest integer in X and the corresponding values of Q_c are

$$2(2+\tau)\, Q_{oc}^2 = \begin{cases} 4\tau\left(\frac{N\tau}{4} - \left\lfloor \frac{N\tau}{4} \right\rfloor\right) & N = 4n \\ 4\tau\left(\frac{N\tau - 1}{4} - \left\lfloor \frac{N\tau - 1}{4} \right\rfloor\right) & N = 4n + 2 \end{cases}$$

To determine multiplicities of the reflections all nodes in Z^{*6} for $n_i \leq 7$ were grouped by their length Q and counted.

Table 1 lists for each N, the largest value of M, the indexes in Z^{*6} and R^{*3}, the multiplicities and the values of Q_o and Q_c. This same table can be used to find those vectors in Z^6 for each S that are closest to being parallel to the plane R^3.

N	M	Coordinates in R6						Coordinates in R3						Mult.	Q Paral.	Q Perp.
0	0	0	0	0	0	0	0	0	0	0	0	0	0	1	0.00000	0.00000
2	1	0	0	1	0	0	0	0	0	1	0	0	1	12	0.70711	0.70711
4	4	0	0	1	0	0	1	0	0	0	0	0	2	30	1.20300	0.74350
6	9	0	1	1	0	0	1	0	1	0	0	1	2	20	1.68572	0.39794
8	12	0	1	1	0	-1	1	0	0	0	0	2	2	30	1.94650	0.45951
10	13	1	1	1	0	-1	1	1	0	0	1	2	2	60	2.07095	0.84329
12	16	1	1	1	1	-1	1	0	0	0	2	2	2	12	2.28825	0.87403
12	16	0	1	2	0	0	1	0	1	1	0	1	3	60	2.28825	0.87403
14	21	0	1	2	0	-1	1	0	0	1	0	2	3	60	2.57497	0.60787
16	24	1	1	2	0	-1	1	1	0	1	1	2	3	60	2.75276	0.64984
18	29	1	1	2	1	-1	1	0	0	1	2	2	3	12	2.99535	0.16693
20	32	0	1	2	0	-1	2	0	0	0	0	2	4	30	3.14950	0.28399
22	33	1	1	2	0	-1	2	1	0	0	1	2	4	120	3.22790	0.76200
24	36	1	1	2	1	-1	2	0	0	0	2	2	4	60	3.37143	0.79589
24	36	0	2	2	0	0	2	0	2	0	0	2	4	20	3.37143	0.79589
26	41	0	2	2	0	-1	2	0	1	0	0	3	4	60	3.57225	0.48889
28	44	1	2	2	0	-1	2	1	1	0	1	3	4	60	3.70246	0.54018
28	44	1	1	3	1	-1	1	0	0	2	2	2	4	12	3.70246	0.54018
30	45	0	1	3	0	-1	2	0	0	1	0	2	5	60	3.76938	0.88983
30	45	1	2	2	1	-1	2	0	1	0	2	3	4	60	3.76938	0.88983
30	45	1	2	2	-1	-1	2	2	1	0	0	3	4	20	3.76938	0.88983
32	48	1	1	3	0	-1	2	1	0	1	1	2	5	120	3.89300	0.91901
32	48	0	2	2	0	-2	2	0	0	0	0	4	4	30	3.89300	0.91901
34	53	1	1	3	1	-1	2	0	0	1	2	2	5	60	4.06815	0.67094
36	56	0	2	3	0	-1	2	0	1	1	0	3	5	120	4.18295	0.70918
38	61	1	2	3	0	-1	2	1	1	1	1	3	5	60	4.34643	0.32942
40	64	1	2	3	1	-1	2	0	1	1	2	3	5	60	4.45407	0.40162
42	65	0	2	3	0	-2	2	0	0	1	0	4	5	60	4.50984	0.81320
44	68	1	2	3	0	-2	2	1	0	1	1	4	5	120	4.61367	0.84504
46	73	1	2	3	1	-2	2	0	0	1	2	4	5	60	4.76239	0.56538
46	73	0	2	3	0	-1	3	0	1	0	0	3	6	60	4.76239	0.56538
48	76	1	2	3	0	-1	3	1	1	0	1	3	6	120	4.86082	0.61028
50	77	1	2	3	1	-1	3	0	1	0	2	3	6	120	4.91198	0.93405
50	77	1	2	3	-1	-1	3	2	1	0	0	3	6	60	4.91198	0.93405
52	84	0	2	3	0	-2	3	0	0	0	0	4	6	30	5.09600	0.17552
54	85	1	2	4	1	-1	2	0	1	2	2	3	6	60	5.14482	0.72856
54	85	1	2	3	0	-2	3	1	0	0	1	4	6	120	5.14482	0.72856
56	88	1	2	3	1	-2	3	0	0	0	2	4	6	60	5.23607	0.76393
56	88	0	3	3	0	-1	3	0	2	0	0	4	6	60	5.23607	0.76393
58	93	1	3	3	0	-1	3	1	2	0	1	4	6	60	5.36757	0.43493
60	96	1	3	3	-1	-1	3	2	2	0	0	4	6	20	5.45509	0.49189
60	96	1	2	4	1	-2	2	0	0	2	2	4	6	60	5.45509	0.49189
62	97	1	2	4	0	-1	3	1	1	1	1	3	7	120	5.50073	0.86137
62	97	0	3	3	0	-2	3	0	1	0	0	5	6	60	5.50073	0.86137
64	100	1	3	3	0	-2	3	1	1	0	1	5	6	120	5.58617	0.89148
64	100	1	2	4	1	-1	3	0	1	1	2	3	7	120	5.58617	0.89148
66	105	2	2	4	1	-2	2	1	0	2	3	4	6	60	5.70961	0.67270
66	105	0	2	4	0	-2	3	0	0	1	0	4	7	60	5.70961	0.67270
68	108	1	2	4	0	-2	3	1	0	1	1	4	7	120	5.79197	0.67312
70	113	1	2	4	1	-2	3	0	0	1	2	4	7	60	5.91112	0.24222
72	116	1	3	4	0	-1	3	1	2	1	1	4	7	60	5.99070	0.33385
72	116	2	2	4	2	-2	2	0	0	2	4	4	6	12	5.99070	0.33385
74	117	1	3	4	1	-1	3	0	2	1	2	4	7	60	6.03229	0.78196
74	117	1	3	4	-1	-1	3	2	2	1	0	4	7	60	6.03229	0.78196
76	120	2	2	4	1	-2	3	1	0	1	3	4	7	120	6.11030	0.81501
76	120	0	3	3	0	-2	3	0	1	1	0	5	7	120	6.11030	0.81501
78	125	1	3	4	0	-2	3	1	1	1	1	5	7	120	6.22336	0.51944
80	128	1	3	4	1	-2	3	0	1	1	2	5	7	120	6.29900	0.56798
80	128	0	2	4	0	-2	4	0	0	0	0	4	8	30	6.29900	0.56798
82	129	2	2	4	2	-2	3	0	0	1	4	4	7	60	6.33856	0.90697
82	129	1	2	4	0	-2	4	1	0	0	1	4	8	120	6.33856	0.90697
84	132	2	2	5	1	-2	2	1	0	3	3	4	7	60	6.41285	0.93562
84	132	2	3	4	0	-2	3	2	1	1	2	5	7	60	6.41285	0.93562
84	132	1	2	4	1	-2	4	0	0	0	2	4	8	60	6.41285	0.93562
84	132	0	3	4	0	-1	4	0	2	0	0	4	8	60	6.41285	0.93562
86	137	2	3	4	1	-2	3	1	1	1	3	5	7	60	6.52066	0.69351
86	137	1	3	4	0	-1	4	1	2	0	1	4	8	120	6.52066	0.69351
88	140	1	3	4	-1	-1	4	2	2	0	0	4	8	60	6.59289	0.73058
88	140	1	2	5	1	-2	3	0	0	2	2	4	8	60	6.59289	0.73058
90	145	2	2	5	2	-2	2	0	0	2	4	4	7	12	6.69781	0.37326
90	145	0	3	4	0	-2	4	0	1	0	0	5	8	60	6.69781	0.37326
92	148	1	3	4	0	-2	4	1	1	0	1	5	8	120	6.76815	0.43830
94	149	2	2	5	1	-2	3	1	0	2	3	4	8	120	6.80499	0.83193
94	149	1	3	4	1	-2	4	0	1	0	2	5	8	120	6.80499	0.83193
94	149	1	3	4	-1	-2	4	2	1	0	0	5	8	60	6.80499	0.83193
96	152	1	3	5	0	-2	3	1	1	2	1	5	8	120	6.87424	0.86307
98	157	1	3	5	1	-2	3	0	1	2	2	5	8	120	6.97492	0.59200
100	160	2	2	5	2	-2	3	0	0	2	4	4	8	60	7.04250	0.63502
100	160	1	4	4	0	-1	4	1	3	0	1	5	8	60	7.04250	0.63502
100	160	0	3	4	0	-3	4	0	0	0	0	6	8	30	7.04250	0.63502
102	165	1	4	4	-1	-1	4	2	3	0	0	5	8	20	7.14081	0.09394
104	168	2	3	5	1	-2	3	1	1	2	3	5	8	60	7.20683	0.24822
106	169	1	4	4	0	-2	4	1	2	0	1	6	8	120	7.24144	0.74941
108	172	1	4	4	-1	-2	4	2	2	0	0	6	8	60	7.30654	0.78384
108	172	1	3	5	1	-3	3	0	0	2	2	6	8	60	7.30654	0.78384
108	172	0	3	5	0	-2	4	0	1	1	0	5	9	120	7.30654	0.78384
110	177	2	3	5	2	-2	3	0	1	2	4	5	8	60	7.40135	0.46901
110	177	1	3	5	0	-2	4	1	1	1	1	5	9	120	7.40135	0.46901
112	180	1	3	5	1	-2	4	0	1	1	2	5	9	120	7.46507	0.52226
114	181	2	3	5	1	-3	3	1	0	2	3	6	8	120	7.49848	0.87907

Table 1

The main distances and/or reflections of the icosahedral quasilattices indexed according to N and M, in Z^6 and in R^3 and in perpendicular space.

VII - PEAK POSITIONS

In figure 1, we compare the experimental diffraction curves with a series of vertical lines at the value of Q_o from N = 2 to N = 106 with none omitted using A = 0.65 nm. Every strong peak attributed to the icosahedral phase coincides with such a position. A few weak peaks were found to line up with the next lower value of M, $M_1 = M_o - 4$. Except for these weak peaks, all peaks fall at angles determined by a single lattice parameter A=0.46nm and one other number N which takes on the value of all positive even integers. In a sense $Q_o(N)$ is the icosahedral equivalent of the crystallographic rules which determine for powder patterns of crystalline materials where the lines are to be found. As for crystalline materials it has a beginning at N = 2, and extends monotonically to higher angles. Strictly any list of all peaks must involve two parameters N and M, and because of the irrational number τ, Q can come infinitesinally close to any angle. Only the main Q_o sequence has high intensity. This is similar to what occurs with incommensurately modulated phases. However, the strong peaks from an incommensurately modulated phase conform to a periodic lattice.

VIII - INTENSITY

We find that the intensity of neutron diffraction differs significantly from that obtained with X-rays. This indicates a degree of chemical ordering. The intensities are not consistent witha concept of a simple superlattice. since there is no systematic intensity difference correlated with aby parity rules on N. In any ordering scheme the N=4u+2 peaks would be superlattice peaks since they all would disappear in any structure that belonged to an icosahedral super group. As in ordinary cryustallography, the positions of the reflections depend entirely on the six dimensional lattice and its parameter, only the intensity is affected by other factors. Because the icosahedral phase exists over a range of compositions, as verified by the shift in lattice parameter, there must be substitutions of manganese and aluminum for each other and a certain degree of chemical disorder. In the simplest models, identical single scatterers concentrated on a quasilattice,/9,10/ neutron and xray diffraction would give similar intensities, which would be a known function only of Q_c. This kind of model is clearly ruled out. More complicated models, involving a quasilattice decorated with identical motifs give rise to a factorable structure factor in which one of the factors gives information about possible quasilattices. This will be discussed next.

VIII - INFERENCE ABOUT THE CUT FUNCTION

A quasiperiodic arrangement of points in R^3 with icosahedral symmetry is easily obtained by projecting all lattice nodes in Z^6 within a symmetric by a neighborhood of the icosahedral plane and projecting them onto the icosahedral plane. The shape of the neighborhood must conform to icosahedral symmetry. The size and shape of the neighborhood is called the cut function. It determines the density and arrangement of quasilattice nodes. It is worth noting that no points in the quasilattice will be separated by X if X_c can not be fit into the cut function. The shape and size of the cut function can be adjusted to eliminate specific distances in the quasilattice. If each quasilattice node is decorated with the same atomic motif then the structure factor of such a structure is the product of two factors, an intrinsic quasilattice structure factor and one derived from the arrangement of atoms in the motif. The former depends entirely on the cut function. The separation into two factors is an approximation. In the ideal structure there is no quasilattice lattice of points which have strictly identical environments. We assume an approximate repetition of local environment, and use the observed intensity to make inferences about the spacing of quasilattice nodes form the size of the cut

function. If we assume that the cut function is a sphere we can obtain the quasilattice structure factor F which is only a function of the dimensionless cut radius R

$$F = 3(\sin\phi/\phi^3 - \cos\phi/\phi^2) \qquad (10)$$

where

$$\phi = 2\pi Q_c R$$

F has zeros at $\phi = 4.49, 7.72...$

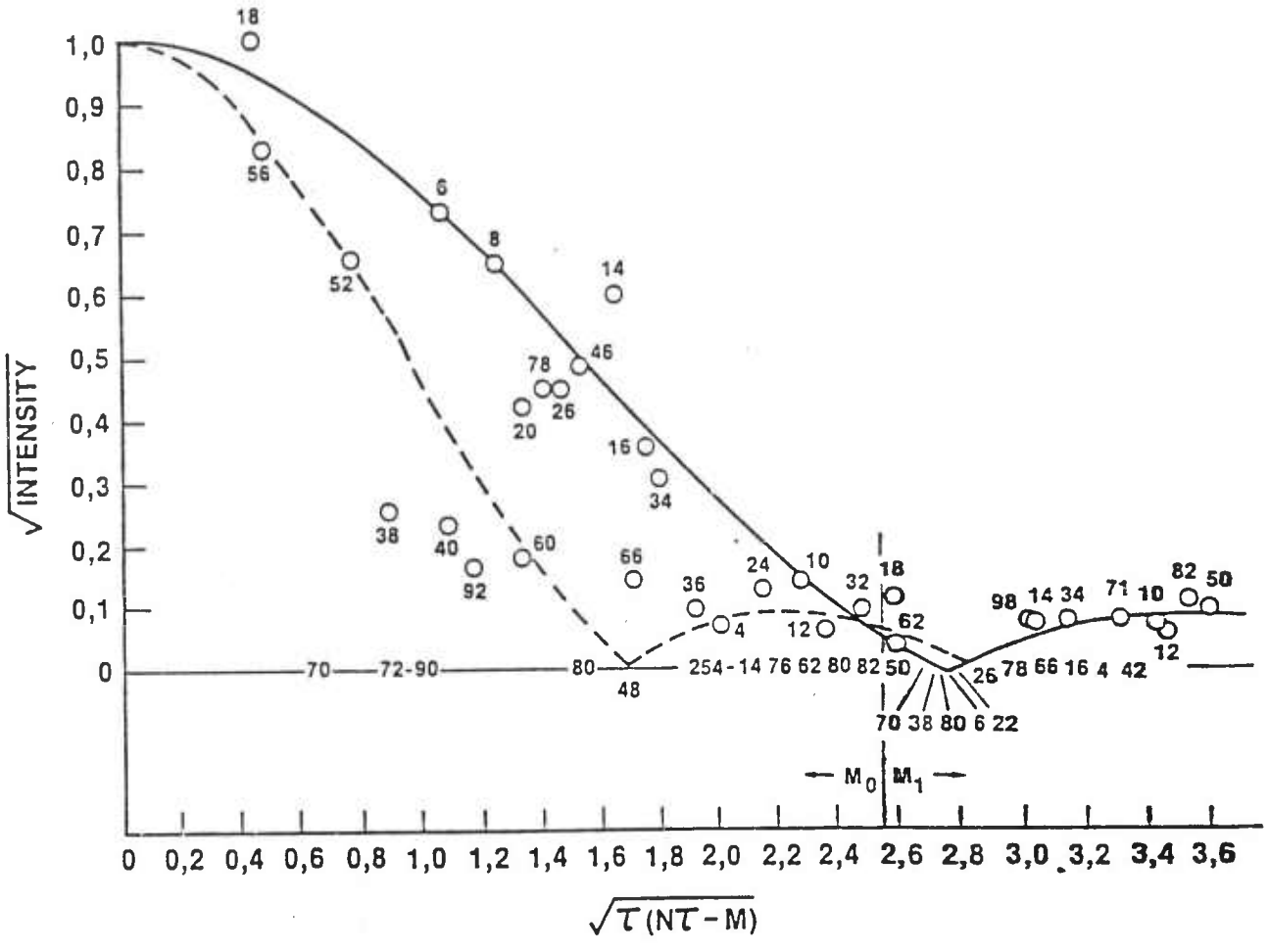

Fig. 3 - The square root of the relative intensity corrected for multiplicity and the Lorentz factor versus $2(2+\tau)\,Q_c$. Both the Q_o and Q_1 series are shown. The value of N is shown for each reflection. Where no peak was observed the intensity was set to zero. The solid and dashed curves are quasilattice structure factors for spherical cuts for R=0.704 and 1.14 respectively. The latter is the sphere with the same volume as the cut figure which gives the three-dimensional Penrose tiling.

Fig. 3 plots intensity vs. $\tau(N\tau-M)$ which is Qc $2(2+\tau)$. The quasilattice structure factor F is plotted for two values of the dimensionless radius of a spherical cut function R=1.14 and R=0.704. The former has a node in Fig. 3 at 1.65, the other at 2.73. The larger R is a sphere of the size of the tri icoutahedron that gives the quasilattice of the 3-dim Penrose tiling. For this size the principal node spacing is 0.46nm along the 5-fold axis, corresponding to S=2, T=1, although it also admits a few of the short diagonals of the oblate tile, S=6 T=-3. Because of the many intense reflections near the node of this structure factor we conclude that this is not the size of the cut function, that these distances are not quasilattice vectors, and that this the observed quasilattice is not represented by the 3-dimensional Penrose filing. The smaller value of R does indeed give a node at 2.73 where there are no intense reflections. This size cut function rules out S=2 and S=4 and all S=6 except T=9, which becomes the shortest distance allowed and is 1.096nm along the 3-fold axis. This is indeed the caliper diameter of a Mackay icosahedron /11/ along its three-fold axis and figures in the model proposed by Henley and Elser/12/, Guyot and Audier,/13/ Ma, Stern, and Bouldin /14/. In such a model parallel Mackay icosahedra are placed on nodes separated by 1.096nm along their common three-fold axis forming distorted octahedra where they join. No nodes are closer than this distance. In another paper we describe the construction of a cut-figure which will give a quasilattice with these properties.

REFERENCES

/1/ D. Shechtman and I. Blech, Met. Trans. 16A, (1985) 1005.
/2/ D. Shechtman, I. Blech, D. Gratias, and J. W. Cahn, Phys. Rev. Lett. 53 (1984) 1951.
/3/ L. Bendersky, R. J. Schaefer, F.S. Biancaniello, W. J. Boettinger, M. J. Kaufman, and D. Shechtman, Scripta Met. 19 (1985) 909.
/4/ R.J Schaefer, L.A. Bendersky, D. Schectman, W.J. Boettinger, and F.S. Biancaniello, Met. Trans. A (to be published).
/5/ L. Bendersky, Phys. Rev. Lett. 55 (1985) 1461.
/6/ E. Prince and A. Santoro, in "National Bureau of Standards, U.S. Technical Note 1117" (F. Shorten, Ed.) (1980)
/7/ P.A. Bancel, P.A. Heiney, P.W. Stephens, A.I. Goldman, and P.M. Horn, Phys. Rev. Lett. 54, (1985) 2422.
/8/ J.W. Cahn, D. Shechtman and D. Gratias J. Mat. Res. 1, (1986) 13.
/9/ M. Duneau and JA. Katz, Phys. Rev. Lett. 54 (1985) 2688.
/10/ V. Elser, Acta Cryst. A 42, (1986) 36
/11/ A.L. Mackay, Acta Cryst. 15, (1962) 916.
/12/ V. Elser and C.L. Henley Phys. Rev. Lett. 55, (1985) 2883.
/13/ P. Guyot and M. Audier, Phil. Mag. B52, (1985) L15.
/14/ Y. Ma, E.A. Stern and C.E. Bouldin, (Submitted to Phys. Rev. Letters).